IDENTIFICATION AND CONTROL OF NONLINEAR DIFFERENTIAL SYSTEMS WITH STICTION AND COULOMB FRICTION

By

WILLIAM FRED ACKER

A DISSERTATION PRESENTED TO THE GRADUATE COUNCIL OF
THE UNIVERSITY OF FLORIDA
IN PARTIAL FULFILLMENT OF THE REQUIREMENTS FOR THE
DEGREE OF DOCTOR OF PHILOSOPHY

UNIVERSITY OF FLORIDA

April, 1967

University of Florida
1853

UNIVERSITY OF FLORIDA
3 1262 08552 2760

ACKNOWLEDGMENTS

I thank all those who helped me obtain the NASA fellowship which paid for the first two years of this four-year effort. That includes two people who helped me obtain the forms, six who wrote letters of recommendation, dozens who processed and approved forms, and millions who paid taxes. There is not room here to mention them all individually, but my gratitude is sincere.

Many fellow Honeywell employees have helped me by arranging a leave of absence and allowing me to work as a part-time employee. A few of those people who helped in special ways are: F. X. Pesuth, G. T. Bynum, M. J. Conway, S. F. Sando, T. M. Berlage, and T. W. Christensen. A particular debt is owed to Dr. E. Tims who triggered my decision to start on this project and showed me how to start. Thanks are also expressed to R. Meredith who came out in the middle of the night on his own time to repair the computer for me, and to many others who were equally helpful in other ways such as Roy Nurse and Leo Spiegel.

A debt is acknowledged to my family which has gotten along on half of my normal income and a tiny fraction of my normal time and attention for the past four years.

I deeply appreciate the cooperative attitude of all of the faculty at Gainesville, particularly the members of my committee. I thank the chairman of my committee, Dr. A. P. Sage, and whole-heartedly recommend him to any graduate student who wants an education in control theory and is willing to work for it.

Thanks are also given to Mrs. Gertrude Wharton, who proofread and typed the final draft of this document.

TABLE OF CONTENTS

Page

ACKNOWLEDGMENTS ii

LIST OF FIGURES v

ABSTRACT vi

Chapter

1 INTRODUCTION 1

2 BACKGROUND AND DEFINITION OF THE PROBLEM . 9

3 DEVELOPMENT OF THE MULTIMODE-LINEARIZATION TECHNIQUE FOR THE PRECISE HIGH-SPEED SIMULATION OF NONLINEAR SYSTEMS 25

4 EXTENSION OF MULTIMODE LINEARIZATION TO INCLUDE STOCHASTIC NOISE 36

5 SOLUTION OF A MULTIMODE-IDENTIFICATION PROBLEM BY USING MODE ESTIMATORS, PARTITIONED AND MODIFIED KALMAN FILTERS, AND BOUNDARY-CONDITION MATCHING 49

6 DEFINING, EVALUATING, AND MINIMIZING THE COST FUNCTION 64

7 THE DIGITAL SIMULATION 72

8 CONCLUSIONS, APPLICATIONS, AND TOPICS FOR FURTHER STUDY 85

KEYED BIBLIOGRAPHY 89

ADDITIONAL BIBLIOGRAPHY 91

BIOGRAPHICAL SKETCH 93

LIST OF FIGURES

Figure		Page
2-1	BLOCK DIAGRAM OF THE NONLINEAR-PLANT MATH MODEL SHOWING THREE PIECEWISE-LINEAR MODES	22
7-1	GREATLY SIMPLIFIED AND ABBREVIATED COMPUTER FLOWCHART	75
7-2	ERROR VERSUS TIME	79
7-3	ERROR VERSUS TIME, CONTINUED	80
7-4	FRICTION ESTIMATES VERSUS TIME	81
7-5	COST AND Δ_c RATIO VERSUS TIME	82

Abstract of Thesis Presented to the Graduate Council
in Partial Fulfillment of the Requirements for the Degree of
Doctor of Philosophy

IDENTIFICATION AND CONTROL
OF NONLINEAR DIFFERENTIAL SYSTEMS
WITH STICTION AND COULOMB FRICTION

By

William Fred Acker
April 22, 1967

Chairman: Dr. A. P. Sage
Major Department: Electrical Engineering

The object of this study is to develop theoretical techniques which will be helpful in designing a more accurate servomechanism in order to control the angular position of an output shaft so as to track a slowly moving reference position. It is assumed that motion is slow enough to excite stick-slip, nonlinear oscillations. The specific application motivating this study is the desire to build more accurate gimbal-position control systems for testing inertial-guidance components; however, the analysis and control techniques are developed and discussed from a general rather than specific point of view. The results are applicable to a wide range of problems.

Using previous results, an inequality is derived which specifies the maximum positional accuracy obtainable with a particular set of plant parameters when using classical, linear, time-invariant control strategies. The assumptions in that derivation are examined, and it

is discovered that they can be circumvented by using semi-open-loop, nonlinear, identification and control strategies; hereafter called, solnic strategies. The solnic strategies are called "semi-open-loop" because an entire corrective-manipulation cycle of the control variable is completed on an open-loop, predictive basis before any feedback concerning the results of those manipulations is received. When feedback information is eventually received, it is used to improve the parameter and state-variable estimates with which the controller predicts the next appropriate sequence of control-variable manipulations; therefore, the control loop is not completely open. As a consequence of the optimization requirements, the control variable is switched rather than controlled linearly. The control process can be no more accurate than the identification process; therefore, great emphasis is placed on the development of an accurate state and parameter estimation technique for highly nonlinear systems.

A discrete simulation technique for noisy nonlinear systems is developed which is at least a thousand times faster than standard, fixed-increment numerical integration for this particular system. Using time domain, piecewise linearization, the nonlinear equations are partitioned into linear sets which are called modes. State-transition matrices are used to update the state variables from mode-switching time to mode-switching time. Boundary conditions are matched, state-transition matrices changed, and noise vectors added at the mode-switching times. A completely general technique for

constructing vector, stochastic samples with the desired variances and covariances from a minimum number of independent, zero-mean unity-variance, Gaussian samples is derived and explained in considerable detail.

The Kalman-filtering technique is modified using the piecewise, multiple-mode linearization approach sketched above; however, nonlinearities remain. Techniques for handling these nonlinearities and for estimating the system mode are discussed and specific solutions presented. The multiple-mode Kalman-filtering technique has such great generality and is so conceptually simple that it has implications much broader than those presented here.

Digital simulations were performed using all of the techniques sketched above. When started with large initial estimation errors, the controller rapidly improves the estimates and converges to an optimal strategy in order to minimize a predefined cost function. It was demonstrated that, by use of the solnic strategy, it is possible to control the angular position of the output shaft with at least an order of magnitude more accuracy, and with less energy than when using classical, time-invariant, linear control strategies. The ultimate accuracy limitation when using a solnic strategy has not yet been determined.

CHAPTER 1

INTRODUCTION

1.1 Motivation

The objective of this study was to develop theoretical techniques which would be helpful in designing a more accurate servomechanism for controlling the angular position of an output shaft so as to track a slowly moving position. It was assumed that the motion would be slow enough to excite stick-slip, nonlinear-frictional oscillations. The application motivating this study was the desire to build more accurate gimbal-position control systems for use in the laboratory testing and calibration of inertial guidance components. The same techniques would also be useful for precision pointing of astronomical telescopes, radar antennas, and machine tools.

Most of the techniques which were developed have far greater generality than would be expected from the narrowness of the stated objective. Actually, a conscientious effort has been made throughout this study and the reporting on this study to generalize as much as possible in order to keep from getting lost in a mass of detail. After all, as R. W. Hamming said, "The purpose of computing is insight, not numbers" (1, p. v). Chapter 4 is a specific example of the effort

spent in generalizing. After the specific solution required for simulating the plant noise used in this study had already been obtained, several weeks were spent developing a completely general technique for doing the same thing. Only the general technique is included in this report. The derivation of the general technique is presented in Chapter 4. The specific solution, which was omitted, is very impressive because it involves contour integration; the formation and integration of joint density functions to obtain marginal variances, conditional variances, and covariances; and the guessing of a particular nonunique solution out of an infinite set. The general solution is much less impressive; in fact, it would be a trivial task to program a digital computer to perform the entire solution automatically. On the other hand, that simplicity is the very thing which makes the general solution much more valuable. It is hoped that enough detail has been omitted that the reader will find "insights, not numbers," and yet that enough detail has been retained to allow him to continue from the point where this study stopped without the need for rediscovering anything.

1.2 Precis

In Chapter 2, an inequality is derived which specifies the maximum accuracy obtainable using classical, linear, time-invariant control techniques for the position control servomechanism with inertia, stiction, and coulomb friction acting at the load. A semi-open-loop, nonlinear, identification and control strategy is then

proposed for breaking the theoretical accuracy bound. The strategy is called "semi-open-loop" because an entire cycle of corrective manipulations of the control variable is completed before any feedback concerning the results of those manipulations is received. Each individual correction cycle is handled on an open-loop predictive basis. The strategy is only semi-open-loop because feedback data is eventually received and used for improving the accuracy of the plant model which is used for estimating the appropriate open-loop actions. The strategy is called nonlinear because the control variable is switched to conserve energy rather than varied proportionally. When stiction is present, the typical linear control will waste large quantities of energy by pushing gently on a shaft which will not come unstuck until a much larger torque is applied. To facilitate communication, the term "semi-open-loop, nonlinear, identification and control strategy" is abbreviated to "solnic strategy."

Having introduced the solnic concept and proposed that concept as a possible means for exceeding accuracy obtainable with classical, linear, time-invariant control strategy for a specific plant, Chapter 2 goes on to define a specific plant. Some of the limitations of the classical, nonlinear friction model are discussed and a more detailed though still imperfect model is constructed. Typical effects which limit the bandwidth of physical plants are mentioned and two are chosen for the plant model. Then, the total plant model is specified in detail.

Chapter 3 presents a new technique for simulating nonlinear systems with a digital computer. The prime prerequisite for using this technique is that it must be possible to approximate the plant by piecewise linearization of the equations in the time domain. The plant model being studied satisfies the piecewise linearization requirement. In fact, as will be shown, the nonlinear plant equations can be partitioned into three sets of linear equations: one set to describe the plant when the output shaft velocity is positive, a second set to describe the plant when the output shaft is stuck, and a third set to describe the plant when the output motion is negative. These three operating conditions are called three plant modes. By partitioning the plant equations into linear modes, determining the times when mode changes occur, solving for the response from mode-switching time to mode-switching time using state-transition matrices, and matching the boundary conditions, the plant dynamics can be simulated with greater accuracy and with less computer time than when using numerical integration. The new simulation technique is called multimode linearization. It was necessary to add extra switching points to account for the times at which the control variable was switched, and it was necessary to develop techniques for determining the mode-switching times; however, the multimode-linearization technique worked very well in the digital simulation. The technique should have wide application, because it was faster and more accurate than numerical integration. Most nonlinear problems can be

approximated, if not represented precisely, by piecewise linearization in the time domain.

The technique developed in Chapter 4 is considered to be a very solid contribution not only to the simulation art but also to practicing error analysts. Using the multimode-linearization technique combined with the fairly standard techniques of computing covariance matrices for noise in linear systems, it should be a trivially simple matter to solve for the statistics of the errors in piecewise-linearizable nonlinear systems. In fact, that is exactly what was done in the simulation of the multimode-modified Kalman filter. The greater contribution is in the second half of the chapter. Instead of simulating the noise by numerical integration using hundreds or thousands of random samples from a normal population, random vectorial samples can be generated to fit any physically realizable covariance matrix using no more samples than the number of components in the vector. The saving in the amount of computer time spent merely in the generation of random samples is in itself extremely significant. As a bonus, there are also the same savings in time and improvements in accuracy which were found when applying the multimode-linearization technique to noise-free problems. The addition of noise alters the switching times at which mode changes occur but a fast, accurate solution to the problem was found.

Once the multimode-linearization technique had been developed for simulating the piecewise linear plant, it was probably inevitable

that an attempt would be made to apply the same multimode-linearization concept to the estimation problem. It was not inevitable, however, that the attempt would be successful. The prime obstacle to the application was the task of estimating which mode the system was in at any specific time. The general optimum solution to the mode estimation problem was not worked out or applied because of the computational difficulties in applying Baye's strategy decision-making techniques in such a highly nonlinear system. A maximum-likelihood decision maker was considered but abandoned because the cost of rejecting truth seemed to be far less than that of accepting falsehood. The decision-making scheme which was finally chosen predicts mode changes using the estimated plant model and rejects data when the time of the data observation is within three standard deviations of a mode-change point. Because of the bandwidth limitation, no usable observations were obtained when the plant was in mode 1 or mode 3. No claims of optimality are made for the strategy; but it is claimed that it took extremely little computer time and space, and that it produced excellent results. Using the predictive mode estimation scheme, it was possible to modify the Kalman-filtering process into two separate parts which were connected by setting the boundary conditions equal at the predicted nominal switching times. The scheme for partitioning and connecting the modified Kalman filters is simple in retrospect when explained in detail; however, it will not be summarized here because of the large number of definitions and simple steps involved.

Because of the complexity and extreme nonlinearity of certain of the filtering equations, it was not feasible to obtain partial derivatives of the observations with respect to the estimated state variables (at some points the derivatives are infinite). As consequence of this nonlinearity, some of the standard-Kalman-filtering equations had to be modified by replacing the partials with quasipartials (first-order partial differences). When sufficient nonlinear constraints are added to make the estimation process convergent for large errors, then the errors eventually become small enough that the linearized error equations become accurate and the modified Kalman filter begins to function optimally.

The task of defining a cost function for the control was trivial, but the task of solving for the optimal strategy analytically presents formidable computational barriers. It was decided to make the control system evaluate cost as it operated, and to make it readjust its strategy periodically in order to operate at minimum cost. The optimization system worked quite well but suffered from what seems to be a universal defect. In order to avoid singularity problems in the plant-identification process, it was necessary to perturb the control strategy slightly about the optimum point and that increased the cost. This will be called the identification singularity versus cost nonoptimality dilemma.

Using all of the techniques just discussed, the stochastic, nonlinear plant and the solnic system were simulated using FORTRAN

programming and an SDS 930 computer. The initial estimates for stiction, coulomb friction, and the control strategy perturbation amplitude were set in error by factors of two from their proper values. All other estimates including that of the optimal corrective action were set to zero. It took about 20 seconds for the solnic system to obtain enough information to compute one set of cost functions and modify its strategy once. At 54 seconds, the solnic system had identified the system parameters within 6 percent, changed strategy 13 more times and had effectively reached steady-state operation at the optimum cost point. The 5 percent estimation error was caused by the identification singularity versus cost nonoptimality dilemma. The estimate for k_s was 5.7 percent low, that for k_c was 1.4 percent high and the effects of the errors effectively cancelled each other for operation near the optimum cost point. The modified-Kalman-filter equations had detected this singularity through estimating the covariance between the errors and had reduced the filter gains accordingly. The k_s estimate had only improved 1 percent in the last 20 seconds. The largest errors were two-sevenths as large as the minimum obtainable error using classical, time-invariant, linear control.

When the cost ratio was changed to charge more for error and less for control effort, stable consistent operation with peak errors an order of magnitude below the classical limit was demonstrated. The original objectives had been attained, and several unplanned by-products had been developed. Simulation work was terminated at this point with no effort being made to find the lower limit.

CHAPTER 2

BACKGROUND AND DEFINITION OF THE PROBLEM

2.1 Motivation

The prime objective of this study was to find a more accurate means of controlling the angular position of a mechanical shaft so as to follow a slowly moving commanded position with minimum error. The theoretical techniques developed herein are by-products of that effort. The application which first motivated this study was the laboratory calibration of inertial-guidance platforms and components such as ESG's (electrically suspended gyros). In a typical application, a series of concentric gimbals are mounted on a cement pier and a set of gyros and accelerometers are mounted in the center of the gimbal system. The angular velocities which the gimbal servo systems must track are relatively constant and seldom much greater than 15 degrees-per-hour. In order to minimize errors in instrument calibration, it is desirable to make the gimbal control servomechanisms as accurate as possible. One of the prime causes of gimbal servo error is nonlinear friction and every effort is made to minimize this friction. In some cases, pressurized oil is pumped into specially designed hydraulic gimbal bearings so that the mechanical parts do not touch but float on an oil film with respect to each other. Even so, nonlinear friction

remains because of the need for conducting electrical power and signals to and from the inertial components. Having failed to eliminate nonlinear friction, the control system designer must learn to minimize the angular error caused by that friction. The error minimization problem would be trivial if all of the equations were linear and well defined. The equations are neither linear nor well defined.

One of the first steps in solving a problem is to define it. In this chapter, the classical definitions of the problem will be reviewed. Then an equation stating the minimum friction-induced angular error for classical, time-invariant, linear controllers will be presented and the physical meaning of that equation discussed. At that point, intuition takes over and a predictive, nonlinear, time-variant control strategy presents itself. The classical error equations, nonlinear friction models, and bandwidth specifications become insufficient with respect to the new concept. The remainder of this chapter is spent in redefining the friction model, choosing a new bandwidth limitation, and defining a specific plant which can be used to test the new strategy.

2.2 Classical Definitions and Solutions

Classically, the friction in servomechanisms is considered to be made up of three components: viscous friction, coulomb friction, and stiction (2, pp. 481-484; 3, pp. 82-83). The magnitude of the torque exerted on the output shaft by viscous friction is equal to a constant times the shaft velocity, and it is in such a direction as to

resist motion. Viscous friction is a linear effect. At the 15 degree-per-hour shaft velocities considered in this study, the effect of viscous friction is negligible.

Stiction and coulomb friction are complementary elements of the classical, nonlinear friction model. When the shaft is moving, stiction torque is zero by definition. When the shaft is stopped, coulomb-friction torque is zero by definition. Let the symbols k_s and k_c represent the stiction coefficient and the coulomb-friction coefficient, respectively. The values of k_s and k_c are positive constants. When the shaft has stopped, then by the definition of stiction, the shaft will not begin to move again until the magnitude of the motive torque exceeds the magnitude of k_s. When the shaft is moving, the coulomb-friction torque is equal in magnitude to k_c and in the proper direction to oppose motion. The ratio of k_s to k_c is never less than unity, and for bearings it is very seldom greater than two.

The magnitude of the static error of a linear servomechanism is equal to the disturbance torque magnitude divided by the static stiffness. In all physical servomechanisms, there is some frequency above which the loop gain must be kept below one. This frequency will be represented by the symbol, ω_b, defined as the bandwidth limit, and discussed in detail later. For an uncompensated linear servomechanism with a pure inertial load, the static stiffness, and hence the static error, is proportional to the square of the system bandwidth. Therefore, the bandwidth limitation is of extreme interest to the servo

designer. For a fixed bandwidth, it is possible to increase the static stiffness by adding a low-frequency lag network to produce integral action (4, pp. 172-209; 5, p. 17). Even if the system is carefully designed to appear conditionally stable under Bode-plot or root-locus analysis, it will oscillate if excessive lag is used and nonlinear friction is present. An excellent article by Bohacek and Tuteur presents a mathematical description of these oscillations in the time domain and derives an inequality limiting the maximum allowable lag ratio (6). The following equation is a free but accurate translation of the Bohacek and Tuteur result when the corner frequencies of the lag network are set low enough that the network does not contribute excessive phase shift at the bandwidth limitation frequency, ω_b.

$$L_{max} = \frac{2k_s}{k_s - k_c} \qquad (2\text{-}1)$$

L_{max} represents the maximum permissible magnitude for the ratio of the two lag network corner frequencies. Attempts to use the describing-function technique in examining the stick-slip oscillations caused by the interaction of lag and nonlinear friction do not yield quantitative accurate results because the waveform is far from sinusoidal (7). The oscillations have been accurately analyzed using phase-plane and phase-space techniques although the task is tedious (8). Fortunately for the reader, it will not be necessary to reproduce either the time-domain or phase-plane analyses. By combining insights from the articles referenced above and a related article by

George Biernson, a simpler derivation can be constructed (9). The maximum accuracy obtainable for a time-invariant linear controller with a bandwidth, ω_b, controlling a load with inertia, J, and non-linear friction coefficients, k_c and k_s, can be derived by inspection. The peak steady-state error, θ_e, of a linear servomechanism as a result of a stiction torque, k_s, is given by

$$\theta_e = \frac{k_s}{S.S.} \tag{2-2}$$

where S.S. represents the static stiffness. For a pure inertial load and a linear control with no compensation,

$$S.S. = J\omega_b^2 \tag{2-3}$$

When lead networks are added to stabilize the system, clearly

$$S.S. \leq J\omega_b^2 \tag{2-4}$$

When the maximum permissible low-frequency integration defined by equation (2-1) is added,

$$S.S. \leq J\omega_b^2 \frac{2k_s}{k_s - k_c} \tag{2-5}$$

Combining equation (2-2) and inequality (2-5)

$$\theta_e \geq \frac{k_s - k_c}{2} \frac{1}{J\omega_b^2} \tag{2-6}$$

Inequality (2-6) gives the minimum obtainable peak error using a time-invariant linear controller under the conditions specified above. The derivation inequality (2-6) by the above process including the derivation of equation (2-1) is a lengthy process punctuated by numerous assumptions. Now the result will be derived by inspection.

Assuming that the load is moving along in a unidirectional manner with stick-slip motion, the frictional torque will oscillate in a sawtooth manner between the magnitude of k_s to that of k_c. When the torque drops instantaneously from magnitude k_s to that of k_c, a step disturbance torque with a peak-to-peak amplitude equal to that of $(k_s - k_c)$ is produced. Below the frequency, ω_b, the servomechanism can respond to counteract the step torque. At the bandwidth frequency the loop gain is unity and the phase angle is usually greater than 90 degrees so the servo is seldom helpful and typically harmful for disturbances of that frequency. Neglecting the efforts of the control system at frequencies equal to and greater than ω_b, the resulting peak error, θ_e, for a sine-wave disturbance torque with a peak-to-peak amplitude equal to that of $(k_s - k_c)$ and a frequency of ω_b acting on a pure inertia, J, is given by

$$\theta_e = \frac{k_s - k_c}{2} \frac{1}{J\omega^2} \qquad (2\text{-}7)$$

The maximum value of θ_e is obtained by setting ω equal to ω_b. The equation is turned into an inequality by examining the waveform of the disturbance torque compared with that of a sine wave. Thus, inequality (2-6) is intuitively obvious--in retrospect. When classical, linear, time-invariant control techniques are applied to the nonlinear friction servomechanism problem, inequality (2-6) states the minimum obtainable peak error. Even if square-wave dither is added to the system, the inequality still stands unless the dither frequency exceeds the bandwidth limitation frequency, ω_b.

2.3 The Classical Control System Versus a Solnic (semi-open-loop, nonlinear, identification and control) System

The weakness of the classical, time-invariant, linear control strategy becomes obvious after examining inequality (2-6). Neither the magnitude of the step torque disturbance, $(k_s - k_c)$, nor the load inertia, J, can be changed by the control designer; the only thing left to change is ω_b, the bandwidth limit. The addition of high-frequency dither is one excellent means for increasing ω_b; however, dither expends control system energy, causes undesirable torque-motor heating, creates noise, and can cause erratic gyro drifts through the effect called "gyro coning."

The irreducible frictional error bound, inequality (2-6), for classical linear controllers results from the fact that these controllers reduce the control effort too slowly once stiction has been overcome and the load begins to move. Ideally, the control effort should be instantaneously reduced to precisely the value of coulomb friction the instant that the load reaches the desired velocity. If this were done precisely and the plant were noiseless, then the load would continue moving at exactly the desired velocity until some change were made. Noise must be added to the plant model to keep this unrealistic solution from appearing. The exact reason for the slowness of time-invariant, linear controllers in reducing the level of the control effort follows as a consequence of the definition chosen for the bandwidth limitation. That definition will be chosen later. However, from an

intuitive point of view, it is obvious that classical, time-invariant, linear controllers respond slowly because they must wait until the optimal linear filters have detected a significant load velocity relative to the noise level before reducing the control effort. Rate networks do not solve the problem because they increase the relative noise to signal ratio.

All that is needed to speed up the reduction of control effort is a little predictive action such as the farmer uses in fertilizing corn. The farmer does not keep pouring ammonia on his corn crop until he sees a change in the corn. He predicts how much ammonia will be required, applies it, and waits for the result. If the result is not satisfactory, he tries a different strategy on the next crop. Most batch processes were controlled in this manner years before the terms control theory, predictive control, or systems science were ever coined. The concept is not new, the context is. Since it is not possible to keep the output shaft of a servomechanism moving continuously at extremely low velocities when stiction, coulomb friction, and frictional noise are present, the new strategy is to abandon continuous, frequency-domain control techniques and treat the problem as a series of batch processes (step corrections) in the time domain.

The new semi-open-loop, identification and control strategy will be called a solnic strategy to save time. It is called semi-open-loop because the entire sequence of corrective commands for a step correction are truly completed before a feedback signal concerning

the results of that correction is received. In the example to be considered, the entire corrective action is completed between the sampling instants of the sample-data-type position error signal. The corrective actions therefore appear to be open loop if looked at within a single corrective cycle; however, the controller gradually identifies the plant by comparing predicted results with observed results. The gradual identification of the plant enables the controller to optimize the heretofore open-loop control sequences, hence the strategy is called a semi-open-loop, identification and control strategy. The word, nonlinear, was added because switched control action was utilized in order to minimize fuel and error costs.

Having outlined the solnic strategy, a general strategy for breaking the classical accuracy limit, inequality (2-5), the remainder of this dissertation is concerned with the development, implementation, and testing of that strategy. One of the objectives is to find out under what conditions, if any, the solnic strategy is superior to the classical, time-invariant, linear strategy. The first three steps toward doing this are: re-examination of friction models, a survey bandwidth limiting factor, and then explicit definition of the plant model to be used for comparison purposes. The remainder of this chapter reports on those three steps.

2.4 The Friction Math Model

The classical math model for friction including viscous friction, coulomb friction, and stiction has already been described. The

necessity of adding noise to the model to prevent a trivial control solution has also been explained. When viscous friction is neglected, and white and correlated friction noises are added, the model becomes essentially that which was chosen for plant model in section 2.6; nevertheless, a few other factors are worth mentioning.

Very little accurate data exists concerning stiction effects for shaft motions of microradian amplitudes and 15 degree-per-hour average velocities; however, on the basis of limited experimentation, it has been possible to build the following picture of the nonlinear friction effects acting in an inertial-platform gimbal structure. First, because of structural flexibilities, small reversible, zero-hysteresis motions occur before any sliding or rolling motion takes place. Second, ball bearings break loose and begin to roll or slide before electrical brushes in the torque motors and resolvers. Third, the ball bearings, torque-motor brushes, and resolver brushes can be moved back and forth through unexpectedly large angles before the electrical "wipers" on the slip rings begin to slide. Fourth, the scores of slip-ring wipers can come unstuck at different times creating a rather stochastic model. Fifth, the two gimbal bearings do not move together; in fact, if a step torque is applied to the torque motor at one bearing, the other bearing may even back up a slight amount before beginning to follow. This reversal effect was not observed until after it was predicted theoretically; it is not obvious either in theory or practice. Sixth, neither k_s nor k_c is constant. Seventh,

magnetic effects within the torque motors are significant. No numbers are given for the above effects because they vary from platform to platform, and the numbers associated with any specific type of platform are frequently considered to be company proprietary.

The above effects are pointed out merely to keep any readers from taking the friction model used herein too literally. The friction model with merely three effects, stiction, coulomb friction, and frictional noise, is considered sufficient for development of the solnic technique. Before attempting to apply the solnic technique to any real physical plant, however, the reader is cautioned to consider the friction model very carefully.

2.5 The Bandwidth Limitation

The bandwidth limitation is a sufficiently broad topic for a rather lengthy discussion. In the following paragraphs only a few of the most salient features of this subject are mentioned.

It was decided that before any bandwidth limitation would be considered for the nonlinear plant math model, it would have to satisfy four requirements. First, it would have to be a limitation which occurs frequently in current practice. Second, the mathematical model of the limitation would have to be simple enough to be mathematically tractable. Third, the mathematical model would have to represent the real physical system accurately enough for the results to be meaningful, at least in a qualitative manner.

Lastly, to facilitate comparison between the linear, time-invariant controller and the nonlinear, time-varying controller, the bandwidth limitation would have to be compatible with the analytical techniques used for synthesizing both types of controllers. Because the solnic concept was still quite nebulous, and because no list of applicable analytical techniques was available, conformance or nonconformance to the last requirement was difficult to assess. What made the problem particularly difficult was that the plant was now not only nonlinear but also stochastic and noisy. Booton's "quasi-linearization" technique was considered but rejected because it does not apply to systems with lag or feedback (10). Fortunately, the desired list of analysis techniques suitable for stochastic, nonlinear control systems was discovered in Pervozvanskii's newly translated book (11, pp. 88-91). Piecewise linearization in the time domain is the analysis technique which was eventually chosen.

Concurrently with the study of analysis techniques, a list of possible bandwidth limitations was prepared and examined. Seven items from that list are worthy of mention here.

1. Transfer functions of miniature, floated, integrating gyroscopes
2. Arbitrary specification of the frequency at which the loop gain equals unity
3. Dead time or transportation lag
4. Limited carrier frequency for the feedback signal

5. Limited sampling rate for the feedback signal

6. Stochastic noise mixed with the feedback signal

7. Variable structural flexibilities

Conformity to precedent demanded the use of limitation 2; however, that limitation was rejected because of the philosophical problems involved in defining the loop gain of a semi-open-loop, nonlinear, identification and control system. Finally, limitation 6 was selected because it seemed to be the one encountered most often in practice. Limitation 5 was also added, which simplifies the task of simulating one of the Kalman filters. The presence of two separate bandwidth limiting factors in the same plant is quite reasonable since most real physical plants have several significant bandwidth limiting effects acting simultaneously.

2.6 Definition of the Plant

The plant model which was selected for study is an ultra-simplified version of the gimbal servo system for an inertial-guidance platform using a sample-data-type error signal. A block diagram of the math model and a mode-switching table is shown in figure (2-1). The switches are in position 1, 2, or 3 depending on the velocity, x_2, and the torque, x_3, as shown by the mode table. The switches mathematically simulate the piecewise-linear behavior of the nonlinear plant. There are no such switches in the real physical plant. The control variable, u(t), represents the voltage applied across the inductive

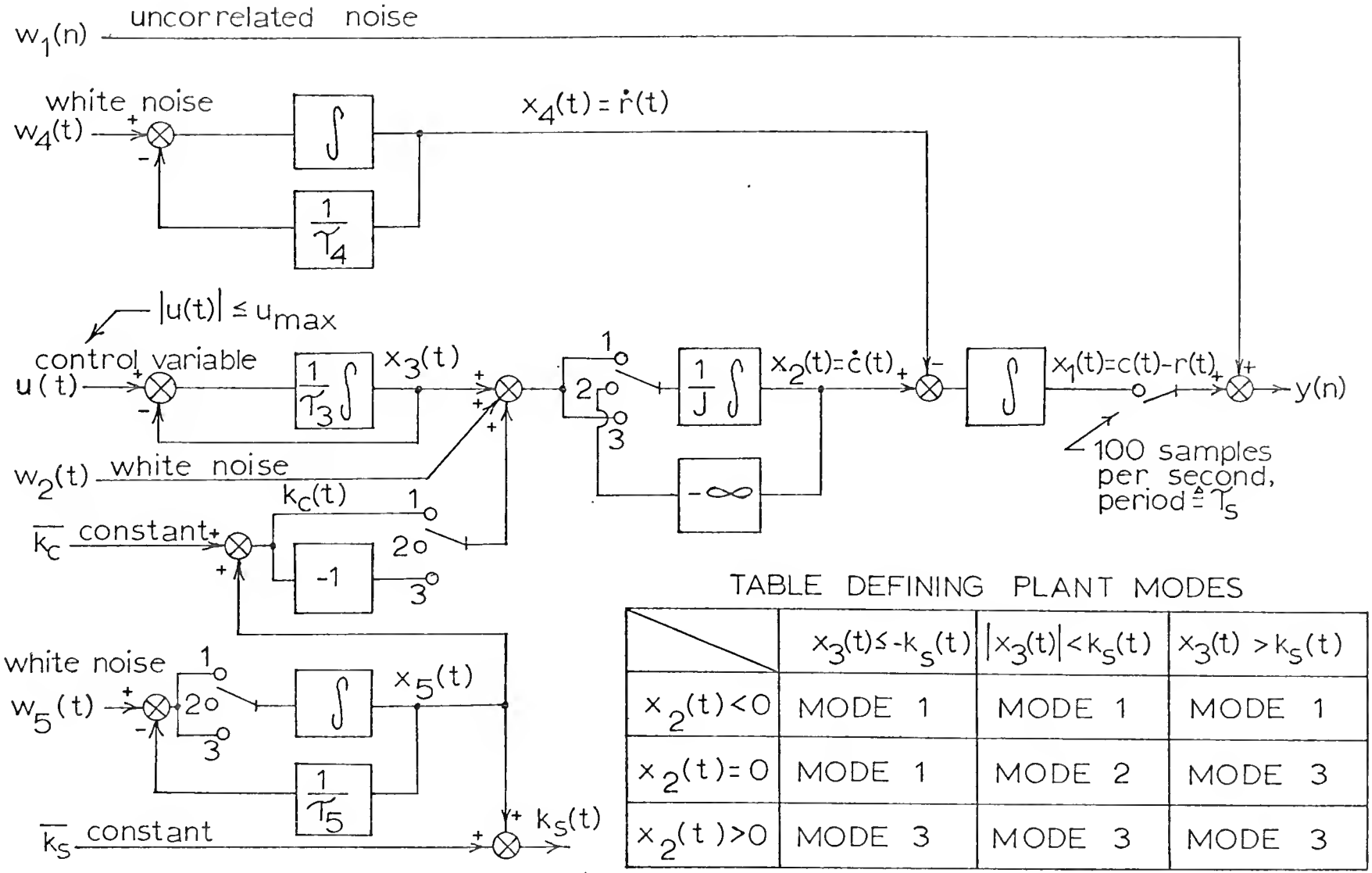

TABLE DEFINING PLANT MODES

	$x_3(t) \le -k_s(t)$	$\lvert x_3(t)\rvert < k_s(t)$	$x_3(t) > k_s(t)$
$x_2(t) < 0$	MODE 1	MODE 1	MODE 1
$x_2(t) = 0$	MODE 1	MODE 2	MODE 3
$x_2(t) > 0$	MODE 3	MODE 3	MODE 3

FIGURE 2-1 BLOCK DIAGRAM OF THE NONLINEAR-PLANT MATH MODEL SHOWING THREE PIECEWISE-LINEAR MODES

coil of the torque motor multiplied by the torque-motor scale factor measured in inch-ounces of torque per volt; thus, $u(t)$ and u_{max} are stated in inch-ounces of torque rather than volts. This normalization eliminates the torque-motor scale factor coefficient from the problem. Notice that $r(t)$ and $c(t)$ are not computed separately and subtracted because that would involve the subtraction of two large numbers to compute a very small one. By subtracting the $\dot{r}(t)$ from $\dot{c}(t)$, full use is made of the computer accuracy and the outputs of all integrators are bounded or have finite variances when the controller is operating.

The infinite-gain feedback path from $x_2(t)$ through the mode switch to $\dot{x}_2(t)$ is merely a reminder that $x_2(t)$ is clamped to zero when the system is in mode 2. Once the math model had been reduced to the three-linear-mode form shown in figure (2-1), the multimode-linearization technique described in the next chapter was an obvious next step in solving the problem.

Before going on to the next chapter, it is necessary to comment on how the magnitudes of the math-model parameters were obtained for table (2-1). The values of J, τm, u_{max}, k_c, and k_s were obtained from unclassified publications by companies other than Honeywell. The value of τ_s is fictitious but plausible. The statistics of x_5 were chosen in the range of earth rate and Schuler oscillations through initial misalignment errors. The statistics of $w_1(n)$ and $x_5(t)$ are fictitious but, hopefully, the reader will find them credible.

Table 2-1

Magnitudes of the Plant Parameters

Description	Symbol	Magnitude
Variance of position measurement noise, $w_1(n)$	$VAR(y-x_1) \triangleq \sigma_1^2$	$\left[5(10)^{-6}\ \text{rad}\right]^2$/sample
Time between samples	τ_s	0.01 sec
Load Inertia	J	0.5 ozf-in-sec^2
Torque-motor time constant	τ_3	$8(10)^{-3}$ sec
Maximum torque	u_{max}	20 ozf-in
Average coulomb-friction torque	$\bar{k}_c \triangleq x_6$	1.4 ozf-in
Average stiction torque	$\bar{k}_s \triangleq x_7$	2.1 ozf-in
Power spectral density of white frictional noise	σ_2^2	$(0.02\ \text{ozf-in})^2$ sec
Power spectral density of white noise, $w_5(t)$	σ_5^2	$1.8(10)^{-4}$ozf^2-in^2-sec
Correlation period of correlated frictional noise	τ_5	1,000 sec
Variance of correlated frictional noise	$VAR(x_5)$	$(0.3\ \text{ozf-in})^2$
Power spectral density of white noise, $w_4(t)$	σ_4^2	$1.8(10)^{-14}$rad^2-sec
Correlation period of commanded velocity	τ_4	1,000 sec
Variance of commanded velocity	$VAR(x_4)$	$\left[3(10)^{-6}\text{rad/sec}\right]^2$

1 ozf $\triangleq$ 1 ounce of force $\triangleq$ 1 ounce mass x 386 in/sec^2

CHAPTER 3

DEVELOPMENT OF THE MULTIMODE-LINEARIZATION TECHNIQUE FOR THE PRECISE HIGH-SPEED SIMULATION OF NONLINEAR SYSTEMS

3.1 Introduction

The ideal equipment for simulating the nonlinear plant and the solnic system would have been a hybrid computer facility with interconnected digital and analog computers. Another fairly good combination would have been to use a general-purpose digital computer for flexible programming, decision making, and control combined with the use of a digital differential analyzer to perform numerical integration. Because of equipment reliability and scheduling problems, it was decided to perform the entire simulation with a single general-purpose SDS 9[illegible] digital computer using the FORTRAN language.

Having decided to perform the simulation using a general-purpose computer, the traditional technique to have chosen would have been numerical integration. The disadvantage of using numerical integration is the speed versus accuracy dilemma. If the time increments for numerical integration are chosen too small, the simulation runs too slowly. If they are chosen too large, the results are inaccurate. Accuracy is not always improved by making the time intervals smaller because the finite word length in the computer causes

roundoff or truncation errors. The multimode-linearization technique was developed while attempting to find the optimum iteration interval to use for the numerical simulation. The unanticipated result was that one should partition the solution into a series of piecewise-linear steps in the time domain and compute from boundary to boundary in single jumps using the appropriate state-transition matrices. The technique is called multimode linearization. The dynamic response of the nonlinear plant is described using a series of linear math models. Each linear math model is called a mode. Only three modes were required to describe the plant defined in figure (2-1). By using a sufficiently large number of modes, it should be possible to approximate almost any real nonlinear plant; therefore, the technique is considered to be quite general.

The advantages of multimode linearization over numerical integration are both speed and accuracy. The multimode-linearization technique is faster because it can step from mode-switching boundary to mode-switching boundary in a single iteration. It is more accurate than numerical integration because it uses an exact, rather than an approximate, set of equations and because the reduction in the number of computations reduces the roundoff errors.

The disadvantages of multimode linearization are that the nonlinear equations must be partitioned into linear modes, the state-transition matrices for these modes must be determined, and mode-switching times must be found. Techniques for partitioning,

determining state-transition matrices, and finding switching times are presented in the remainder of this chapter.

3.2 Partitioning the System Equations

The math model for the plant which is to be simulated is defined by figure (2-1) and table (2-1). The plant equations have already been partitioned into three linear modes. All of the noise sources are denoted by the small letter, w, with various numerical subscripts. In this chapter, stochastic effects are ignored so the magnitudes of all of the noise sources are assumed to be zero. (The effects of the noise will be considered in the next chapter.) The plant state vector contains seven scalars denoted by the small letter, x, with various numerical subscripts. For any time period during which the control effort, u(t), remains equal to zero, the plant equations are linear and homogeneous so the magnitude of the plant state vector at the end of that period may be determined by multiplying its initial magnitude by the appropriate state-transition matrix. If u(t) were always equal to zero, the simulation problem would be trivial.

If the control system for the nonlinear plant is optimized, then the control effort, u(t), will be switched rather than varied continuously. As stated previously, the control effort, u(t), is a normalized measurement of the voltage applied across the coils of a d-c, gimbal torque motor. The torque applied to the friction-inertia load is proportional to the torque-motor current, which in turn follows the applied

voltage but lags behind because of the torque-motor inductance. The cost of the control effort is measured in ampere-seconds divided by the time over which the cost is measured; therefore, the cost is proportional to the average current. By applying "the optimality principle," it may be shown that the control strategy must be piecewise optimal in the time domain. It has already been stated that the new strategy requires that the load be moved in a series of steps rather than continuously. Assuming that the size and frequency of the steps are determined at a higher level in the control hierarchy, the local optimization problem is obviously that of moving the load a given distance with a minimum number of coulombs from the power supply. Application of Pontryagin's maximum principle, indicates that the motor must be switched rather than operated linearly. This answer is intuitively obvious to anyone who has designed class A, B, C and X power amplifiers. Power dissipated in an amplifier is power wasted.

Now that the decision has been made to control the torque-motor voltage with switches, a new problem arises. Something must be done to control the inductive voltage across the torque motor when the switches are opened. One efficient and practical solution is to connect diodes between the inductive coil and the power supply so that the inductive energy is returned to the power supply and so that voltage across the torque motor reverses direction but changes very little in magnitude when the turn-off transient occurs. Neglecting the voltage drops across the diodes and switches, only three values of torque-

motor voltage need be considered in the simulation. The normalized equivalents of these three voltages are: $+u_{max}$, zero, and $-u_{max}$.

Since it has been established that the control effort has three discrete values, a simplification becomes possible. The control variable, u(t), can be thought of as a state-variable which is piecewise constant. Points in time at which u(t) changes from one level to another can be treated in the same manner as points at which plant mode changes occur. Now that the only nonzero-valued forcing function, u(t), has been absorbed into the state vector, the system may be described by equations which are linear with no forcing functions between any consecutive switching points. Under these conditions, state-transition matrices may be used to give the complete solutions. (Later, when the particular solutions for noise are determined, they will be added to the homogeneous solutions. In this chapter, noise is assumed to be equal to zero.)

It is now possible to state the plant equations concisely in matrix form.

To simplify notation, several new symbols will be defined.

$$\alpha \triangleq 1/J \tag{3-1}$$

$$\beta_3 \triangleq 1/\tau_3 \tag{3-2}$$

$$\beta_4 \triangleq 1/\tau_4 \tag{3-3}$$

$$\beta_5 \triangleq 1/\tau_5 \tag{3-4}$$

$$\underline{X(t)} \triangleq \begin{bmatrix} x_1(t) \\ x_2(t) \\ x_3(t) \\ x_4(t) \\ x_5(t) \\ x_6 \\ u(t) \end{bmatrix} \tag{3-5}$$

Notice that x_7 has been omitted since it is constant, and it affects $\underline{X(t)}$ only at the switching times.

Let F_i be defined such that when the plant is in mode i (where i equals 1, 2, or 3) and u(t) is constant during the time interval which the equation is written for, then

$$\dot{\underline{X(t)}} = F_i \, \underline{X(t)} \tag{3-6}$$

The elements of the matrices F_1, F_2, and F_3 may be determined by inspection of figure (2-1).

$$F_1 = \begin{bmatrix} 0 & 1 & 0 & -1 & 0 & 0 & 0 \\ 0 & 0 & \alpha & 0 & \alpha & \alpha & 0 \\ 0 & 0 & -\beta_3 & 0 & 0 & 0 & \beta_3 \\ 0 & 0 & 0 & -\beta_4 & 0 & 0 & 0 \\ 0 & 0 & 0 & 0 & -\beta_5 & 0 & 0 \\ 0 & 0 & 0 & 0 & 0 & 0 & 0 \\ 0 & 0 & 0 & 0 & 0 & 0 & 0 \end{bmatrix} \tag{3-7}$$

$$F_2 = \begin{bmatrix} 0 & 1 & 0 & -1 & 0 & 0 & 0 \\ 0 & -\infty & 0 & 0 & 0 & 0 & 0 \\ 0 & 0 & -\beta_3 & 0 & 0 & 0 & \beta_3 \\ 0 & 0 & 0 & -\beta_4 & 0 & 0 & 0 \\ 0 & 0 & 0 & 0 & 0 & 0 & 0 \\ 0 & 0 & 0 & 0 & 0 & 0 & 0 \\ 0 & 0 & 0 & 0 & 0 & 0 & 0 \end{bmatrix} \qquad (3\text{-}8)$$

$$F_3 = \begin{bmatrix} 0 & 1 & 0 & -1 & 0 & 0 & 0 \\ 0 & 0 & \alpha & 0 & -\alpha & -\alpha & 0 \\ 0 & 0 & -\beta_3 & 0 & 0 & 0 & \beta_3 \\ 0 & 0 & 0 & -\beta_4 & 0 & 0 & 0 \\ 0 & 0 & 0 & 0 & -\beta_5 & 0 & 0 \\ 0 & 0 & 0 & 0 & 0 & 0 & 0 \\ 0 & 0 & 0 & 0 & 0 & 0 & 0 \end{bmatrix} \qquad (3\text{-}9)$$

3.3 Derivation of the State-Transition Matrices

The following equation will be tested to see if it is a solution to equation (3-6). It is often called the matrizant equation, but it also has other names (12, Vol. 2, pp. 149-160).

$$\underline{X(t)} = \left[I + \int_{t_o}^{t} F(z_1)\, dz_1 + \int_{t_o}^{t} \int_{t_o}^{z_1} F(z_1)\, F(z_2)\, dz_1\, dz_2 + \int_{t_o}^{t} \int_{t_o}^{z_1} \int_{t_o}^{z_2} F(z_1)\, F(z_2)\, F(z_3)\, dz_1\, dz_2\, dz_3 + \ldots \right] \underline{X(t_o)} \qquad (3\text{-}10)$$

Differentiating both sides of equation (3-10) with respect to t yields

$$\dot{\underline{X(t)}} = \left[0 + F(t) + F(t) \int_{t_o}^{t} F(z_2)\, dz_2 + F(t) \int_{t_o}^{t} \int_{t_o}^{z_2} F(z_2)\, F(z_3)\, dz_2\, dz_3 \right] \underline{X(t_o)} \qquad (3\text{-}11)$$

Reducing subscripts of z by one,

$$\dot{\underline{X(t)}} = F(t) \left[I + \int_{t_o}^{t} F(z_1)\, dz_1 + \int_{t_o}^{t} \int_{t_o}^{z_1} F(z_1)\, F(z_2) \ldots \right] \underline{X(t_o)} \qquad (3\text{-}12)$$

Substituting equation (3-10) into (3-12)

$$\dot{\underline{X(t)}} = F(t)\, \underline{X(t)} \qquad (3\text{-}13)$$

Thus, it may be seen that equation (3-10) is a solution to equation (3-6) when the F matrix is a function of time. During the time between any two switching points, the F matrix is constant. Let this constant matrix be denoted by F_i where i equals 1, 2, or 3. Then equation (3-10) can be simplified as follows assuming that t_o is the time of the first switching and that t is less than or equal to the time of the next switching.

$$\underline{X(t)} = \left[I + F_i \int_{t_o}^{t} dz_1 + F_i\, F_i \int_{t_o}^{t} \int_{t_o}^{z_1} dz_1\, dz_2 + \ldots \right] \underline{X(t_o)}$$

$$= \left[I + F_i\, h + \frac{(F_i\, h)^2}{2!} + \ldots + \frac{(F_i\, h)^n}{n!} + \ldots \right] \underline{X(t_o)}$$

$$\text{where } h \triangleq (t - t_o) \qquad (3\text{-}14)$$

Define

$$(e)^{F_i h} \triangleq \sum_{n=1}^{n=\infty} \frac{(F_i h)^n}{n!} \tag{3-15}$$

then equation (3-14) may be written more concisely as follows

$$\underline{X(t)} = (e)^{F_i h} \underline{X(t_o)} \tag{3-16}$$

For notational convenience, the three desired state-transition matrices will be represented by the symbols $\bar{\Phi}_1(h)$, $\bar{\Phi}_2(h)$, and $\bar{\Phi}_3(h)$ where the subscript numbers correspond with the mode numbers.

$$\bar{\Phi}_i \triangleq (e)^{F_i h}$$

$$\text{where } i = 1,\ 2,\ \text{or } 3 \tag{3-17}$$

A time when either the plant-mode-description numbers, i, or the control effort level, u(t), changes is defined as a switching time. Let t_n represent any arbitrarily chosen switching time, let t_{n+1} represent the next consecutive switching time, and let i_n represent the plant-mode number between those two switching times. Then

$$\underline{X(t_{n+1}^-)} = \bar{\Phi}_{i_n}(t_{n+1} - t_n)\ \underline{X(t_n^+)} \tag{3-18}$$

Note also that $\underline{X(t_n^+)}$ will always be equal to $\underline{X(t_n^-)}$ except for u(t) which is the only element of $\underline{X(t)}$ that can change by a finite amount in zero time. Once $\bar{\Phi}_1(h)$, $\bar{\Phi}_2(h)$, and $\bar{\Phi}_3(h)$ have been determined, equation (3-18) can be used for the plant simulation. The elements of the state-transition matrices may be determined by computing the first several terms of the series in equation (3-15) and then finding the closed form solution by mathematical induction. Sometimes it is easier to determine the elements by use of Laplace transforms.

$$\Phi_i(h) = \mathcal{L}^{-1}\left[(Is - F_i)^{-1}\right] \tag{3-19}$$

The series expansion method was used to obtain the results shown in equations (3-20), (3-21), and (3-22).

$$\Phi_1(h) = \begin{bmatrix} 1 & h & q_{13} & q_{14} & q_{15} & \alpha h^2/2 & q_{17} \\ 0 & 1 & q_{23} & 0 & q_{25} & \alpha h & q_{27} \\ 0 & 0 & q_{33} & 0 & 0 & 0 & q_{37} \\ 0 & 0 & 0 & q_{44} & 0 & 0 & 0 \\ 0 & 0 & 0 & 0 & q_{55} & 0 & 0 \\ 0 & 0 & 0 & 0 & 0 & 1 & 0 \\ 0 & 0 & 0 & 0 & 0 & 0 & 1 \end{bmatrix} \tag{3-20}$$

where,

$$q_{13} = \alpha\beta_3^{-2}\left[\exp(-\beta_3 h) - 1 + \beta_3 h\right]$$

$$q_{23} = \alpha\beta_3^{-1}\left[1 - \exp(-\beta_3 h)\right]$$

$$q_{33} = \exp(-\beta_3 h)$$

$$q_{14} = -\beta_4^{-1}\left[1 - \exp(-\beta_4 h)\right]$$

$$q_{44} = \exp(-\beta_4 h)$$

$$q_{15} = \alpha\beta_5^{-2}\left[\exp(-\beta_5 h) - 1 + \beta_5 h\right]$$

$$q_{25} = \alpha\beta_5^{-1}\left[1 - \exp(-\beta_5 h)\right]$$

$$q_{55} = \exp(-\beta_5 h)$$

$$q_{17} = \alpha\beta_3^{-2}\left[1 - \beta_3 h + \frac{1}{2}\beta_3^2 h^2 - \exp(-\beta_3 h)\right]$$

$$q_{27} = \alpha\beta_3^{-1}\left[\exp(-\beta_3 h) - 1 + \beta_3 h\right]$$

$$q_{37} = \left[1 - \exp(-\beta_3 h)\right]$$

$\Phi_3(h)$ = Same as $\Phi_1(h)$ except that the four terms inside of the dotted line are multiplied by -1. (3-21)

$$\Phi_2(h) = \begin{bmatrix} 1 & 0 & 0 & q_{14} & 0 & 0 & 0 \\ 0 & 0 & 0 & 0 & 0 & 0 & 0 \\ 0 & 0 & q_{33} & 0 & 0 & 0 & q_{37} \\ 0 & 0 & 0 & q_{44} & 0 & 0 & 0 \\ 0 & 0 & 0 & 0 & 1 & 0 & 0 \\ 0 & 0 & 0 & 0 & 0 & 1 & 0 \\ 0 & 0 & 0 & 0 & 0 & 0 & 1 \end{bmatrix} \qquad (3\text{-}22)$$

where the q's are the same as defined previously.

3.4 Comments Concerning the Technique Implementation

Equations (3-20) and (3-21) are so similar that when the computer program was written the mode 1 and mode 3 update operations were performed with the same subroutine. The equations for mode 2 are so simple that no subroutine was written for that mode.

The problem of determining the switching times was complicated by the stochastic noise. The solutions will be stated in section 4.5. The problem of defining switching boundaries and system "states" (modes) has been treated with great mathematical detail in a recent article by H. S. Witsenhausen which is recommended reading for anyone wishing to pursue the subject further (13).

CHAPTER 4

EXTENSION OF MULTIMODE LINEARIZATION TO INCLUDE STOCHASTIC NOISE

4.1 Introduction

The multimode-linearization technique developed in the preceding chapter is faster and more accurate than numerical integration for simulating the deterministic portion of the plant model defined by figure (2-1). In this chapter, the multimode-linearization technique is extended to include the simulation of the same plant with the effects of stochastic noise added. An even greater saving of computer time occurs when numerical integration is replaced by multimode linearization when stochastic noise is present in the model. The prime reason for this saving is that fewer noise samples are needed, and it takes a fairly large number of computer operations to generate a single normally distributed noise sample.

Since the multimode-linearization technique describes the plant with equations which are linear between switching points, the principle of superposition may be applied to solutions of the equations over the time intervals between switching points. Using this superposition principle, the effect of the noise will be determined in this chapter and simply added to the deterministic solutions obtained in the previous chapter. The noise simulation problem is solved in two

parts. First, the state-vector statistics are computed. Then, vector noise samples with these statistics are generated. The technique is sufficiently general that vector noise samples can be generated to fit any physically realizable covariance matrix. The elements of the vectors are normally distributed with zero means.

4.2 Derivation of the Statistics of the Particular State-Vector Solutions for Stochastic Driving Functions

When the noise vector $\underline{W}$ is defined as follows, the complete solution for the state vector may be written in a simple form.

$$\underline{W(t)} \triangleq \begin{bmatrix} 0 \\ \alpha w_2(t) \\ 0 \\ w_4(t) \\ w_5(t) \\ 0 \\ 0 \end{bmatrix} \tag{4-1}$$

Adding the noise vector $\underline{W(t)}$ to equation (3-6) yields

$$\dot{\underline{X(t)}} = F_i \underline{X(t)} + \underline{W(t)} \tag{4-2}$$

It may be readily verified by differentiation that the complete solution to equation (4-1) may be obtained by adding a convolution integral to the solution given in equation (3-18).

$$\underline{X(t_{n+1}^-)} = \bar{\Phi}_{in}(t_{n+1} - t_n)\, \underline{X(t_n^+)} + \int_{t_n^+}^{t_{n+1}^-} \bar{\Phi}_{in}(t_{n+1}^- - v)\, \underline{W(v)}\, dv \tag{4-3}$$

For brevity, define

$$\underline{N(n)} = \int_{t_n^+}^{t_{n+1}^-} \Phi_{i_n}(t_{n+1}^- - v)\ \underline{W(v)}\ dv \qquad (4\text{-}4)$$

Clearly $\underline{N(n)}$ is the stochastic component which must be added to the deterministic solution given by equation (3-18) in order to obtain the complete solution for the state vector. Assume that the outputs of the separate white-noise sources are uncorrelated, with zero means, and the finite variances specified in table (2-1).

By taking the expected value of both sides of equation (4-4), it may be easily shown that the mean of $\underline{N(n)}$ is equal to zero (all elements of the vector equal zero).

$$\text{MEAN}\left[\underline{N(n)}\right] = E\left[\underline{N(n)}\right] = \underline{0} \qquad (4\text{-}5)$$

For notational compactness, the symbol, E_{ij}, and the term "ij element matrix" will be used to represent a matrix of appropriate dimensions in which the element in the ith row and j^{th} column is equal to unity and all other elements are zeros. The letter, E, without subscripts represents the statistical expectation operation. The transpose of a matrix or vector will be denoted by an apostrophe. For example, the transpose of F will be represented by F'. Then

$$E\left[\underline{W(t_1)}\ \underline{W(t_2)}'\right] = Q\,\delta(t_1 - t_2) \qquad (4\text{-}6)$$

where

$$Q \triangleq E_{22}\,\alpha^2\,\sigma_2^2 + E_{44}\,\sigma_4^2 + E_{55}\,\sigma_5^2 \qquad (4\text{-}7)$$

and $\delta(\ .\ .\ .\ )$ represents the Dirac-delta function.

$$\mathrm{COV}\left[\underline{N(n)}\right] = E\left[\underline{N(n)}\ \underline{N(n)}'\right]$$

$$= E\left[\int_{t_n^+}^{t_{n+1}^-}\int_{t_n^+}^{t_{n+1}^-} \Phi_{i_n}(t_{n+1}^- - u)\ \underline{W(u)}\ \underline{W(v)}'\ \Phi_{i_n}(t_{n+1}^- - v)'\ du\ dv\right]$$

$$= \int_0^h \Phi_{i_n}(v)\ Q\ \Phi_{i_n}(v)'\ dv \qquad (4\text{-}8)$$

$$h \triangleq t_{n+1} - t_n$$

Equation (4-8) is the general solution. To evaluate the elements of the covariance matrix for the plant defined by figure (2-1), it is convenient to separate equation (4-8) into three terms.

$$\mathrm{COV}\left[\underline{N(n)}\right] = \alpha^2\ \sigma_2^2 \int_0^h \Phi_{i_n}(v)\ E_{22}\ \Phi_{i_n}(v)'\ dv$$

$$+\ \sigma_4^2 \int_0^h \Phi_{i_n}(v)\ E_{44}\ \Phi_{i_n}(v)'\ dv$$

$$+\ \sigma_5^2 \int_0^h \Phi_{i_n}(v)\ E_{55}\ \Phi_{i_n}(v)'\ dv \qquad (4\text{-}9)$$

The covariance matrix may be evaluated to any desired degree of accuracy by hand, but the digital computer chosen for the simulation is only accurate to about 9 decimal digits. By neglecting terms which do not affect the six most significant figures, the following approximate (only good to one part per million) solution was obtained for $\mathrm{COV}\left[\underline{N(n)}\right]$ using the mode 1 state-transition matrix defined by equation (3-20).

For mode 1,

$$\mathrm{COV}\left[\underline{N(n)}\right] = \alpha^2 \sigma_2^2 \left[E_{11} \frac{h^3}{3} + (E_{12} + E_{21}) \frac{h^2}{2} + E_{22}\, h\right]$$

$$+ \sigma_4^2 \left[E_{11} \frac{h^3}{3} - (E_{14} + E_{41}) \frac{h^2}{2} + E_{44}\, h\right]$$

$$+ \sigma_5^2 \left[E_{11} \frac{\alpha^2 h^5}{20} + (E_{12} + E_{21}) \frac{\alpha h^4}{8}\right.$$

$$+ (E_{15} + E_{51}) \frac{\alpha h^3}{6} + E_{22} \frac{\alpha^2 h^3}{3}$$

$$\left. + (E_{25} + E_{52}) \frac{\alpha h^2}{2} + E_{55}\, h\right] \qquad (4\text{-}10)$$

For mode 2,

$$\mathrm{COV}\left[\underline{N(n)}\right] = \sigma_4^2 \left[E_{11} \frac{h}{3} - (E_{14} + E_{41}) \frac{h^2}{2} + E_{44}\, h\right] \qquad (4\text{-}11)$$

For mode 3,

$\mathrm{COV}\left[\underline{N(n)}\right]$ = Same as for mode 1, except that the signs of the E_{15}, E_{51}, E_{25}, E_{52} terms are negative (4-12)

It is interesting to note that if the compact element-matrix notation had not been used, equation (4-10) would take up a whole typewritten page. The distributions of the elements of $\underline{N(n)}$ are normal because they are assumed to be generated by Wiener processes; hence, their statistics have been completely determined.

4.3 Generation of Stochastic Vectorial Samples in Accordance with any Physically Realizable Covariance Matrix

The objective is to generate stochastic vectors $\underline{N(i)}$ such that the elements of $\underline{N(i)}$ are normally distributed with means equal to zero and that for any prespecified realizable covariance matrix C,

$$\mathrm{COV}\left[\underline{N(i)}\right] = C \tag{4-13}$$

Presume the existence of a source of independent normally distributed samples with mean equal to zero and variance equal to unity. Construct vectors, $\underline{Z(i)}$, the elements of which are randomly chosen from the uncorrelated, zero-mean, unity-variance, normally distributed population. Find a matrix, A (not necessarily square) such that when vectors, $\underline{N(i)}$, are generated as follows, they will fulfill all of the requirements given in the preceding paragraph.

$$\underline{N(i)} = A\,\underline{Z(i)} \tag{4-14}$$

The elements of $\underline{N(i)}$ fulfill the requirement that they be normally distributed because they are constructed by performing linear operations on normally distributed random variables. Taking the expectation of both sides of equation (4-14)

$$\mathrm{MEAN}\left[\underline{N(i)}\right] = E\left[\underline{N(i)}\right] = A\,E\left[\underline{Z(i)}\right] = A\,\underline{0} = \underline{0} \tag{4-15}$$

Hence, the first two of the three requirements are readily satisfied. Satisfying the third requirement is not quite so trivial.

$$\begin{aligned}\mathrm{COV}\left[\underline{N(i)}\right] &= E\left[\underline{N(i)}\,\underline{N(i)}'\right] = E\left[A\,\underline{Z(i)}\,\underline{Z(i)}'\,A'\right] \\ &= A\,E\left[\underline{Z(i)}\,\underline{Z(i)}'\right]A' = A\,A'\end{aligned} \tag{4-16}$$

Now the problem is reduced to that of finding a matrix A, which is not necessarily square, such that

$$A A' = C, \text{ a specified positive-semi-definite matrix} \quad (4\text{-}17)$$

But there is an infinite number of solutions. For example, if A_o is one solution and G is any orthogonal matrix of appropriate order then $A_o G$ is another solution, which may be proven as follows. By the definition of orthogonality,

$$G' = G^{-1} \quad (4\text{-}18)$$

$$\begin{aligned} COV\left[(A_o G)\,\underline{Z(i)}\right] &= A_o G\, E\left[\underline{Z(i)}\,\underline{Z(i)'}\right] G' A_o' \\ &= A_o G I G^{-1} A_o' = A_o A_o' \triangleq C \end{aligned} \quad (4\text{-}19)$$

Therefore, there are at least as many solutions as there are orthogonal matrices of appropriate order, which means that there are infinitely many solutions. The multiplicity of solutions hinders rather than helps in the effort to find one general solution. The problem was to find a set of constraints sufficient to insure that the solution is always unique, without constraining the problem so much that no solution exists. Also, the solution should be in a form which minimizes the computer time required for generating the vectors, $\underline{N(i)}$. After some study, the following solution was found.

$$\underline{N(i)} = R B \underline{Z(i)} \triangleq A \underline{Z(i)} \quad (4\text{-}20)$$

The constraints are that: R is a rectangular matrix of order n x m with only zeros and ones for elements which are chosen so that

$$R' R = I, \text{ an } m \times m \text{ identity matrix} \quad (4\text{-}21)$$

B is an m x m triangular matrix with elements b_{ij}

$$b_{ij} = 0 \text{ for } i > j \quad (4\text{-}22)$$

$$b_{ij} > 0 \text{ for } i = j \quad (4\text{-}23)$$

The reasons for choosing the constraints this way will become obvious. The R matrix is used to reduce the n x n, positive-semi-definite covariance matrix, C, to the m x m positive-definite matrix, D. The constraint in equation (4-21) simplifies the arithmetic. The constraint in equation (4-22) plus the reduction of C to D minimizes the number of terms which must be included in the computer program. Equation (4-23) is the additional constraint required to make the solution unique. If equation (4-20) is to satisfy equation (4-13), then

$$\mathrm{COV}\left[R\,B\,\underline{Z(i)}\right] = C \tag{4-24}$$

$$R\,B\,B'\,R' = C \tag{4-25}$$

$$R'\,R\,B\,B'\,R'\,R = R'\,C\,R \triangleq D \tag{4-26}$$

$$B\,B' = D, \text{ a positive-definite matrix} \tag{4-27}$$

One definition of R which satisfies the above requirements is

$$R \triangleq \sum_{i=1}^{i=m} E_{k(i)i}$$

where

$E_{k(i)i}$ is an n x m element matrix,

and

k(i) is the index number of the ith nonzero row of C

m is chosen equal to the number of nonzero rows in C.

(4-28)

Other trivially different R matrices may be defined by permuting the columns of the R matrix defined above. Notice that when C is positive definite, R becomes an identity matrix.

Now, the procedure for computing B will be derived. The small letters, r and c, will be used as subscripts to denote row and column index numbers, respectively. Equations (4-27), (4-22), and (4-23) will be used in that order.

$$d_{rc} = \sum_{j=1}^{j=\min(r,c)} b_{rj}\, b_{jc} \tag{4-29}$$

$$d_{11} = b_{11}\, b_{11}$$

$$b_{11} = \text{positive } \sqrt{d_{11}} \tag{4-30}$$

$$d_{r1} = b_{r1}\, b_{11}$$

$$b_{r1} = \frac{d_{r1}}{b_{11}}, \quad r = 2, 3, \ldots, m \tag{4-31}$$

$$d_{22} = b_{21}\, b_{21} + b_{22}\, b_{22}$$

$$b_{22} = \text{positive } \sqrt{d_{22} - b_{21}^2} \tag{4-32}$$

$$d_{rc} = b_{rc}\, b_{cc} + \sum_{j=1}^{c-1} b_{rj}\, b_{cj}, \quad 1 < c \leq r$$

$$b_{rc} = \frac{d_{rc} - \sum_{j=1}^{c-1} b_{rj}\, b_{cj}}{b_{cc}}, \quad 1 < c < r \tag{4-33}$$

$$b_{cc} = \text{positive } \sqrt{d_{cc} - \sum_{j=1}^{c-1} b_{cj}^2}, \quad 1 < c = r \tag{4-34}$$

Equations (4-29) through (4-34) were derived after studying some similar equations in a book by V. N. Faddeeva (14, pp. 81-82). Using

these equations, the triangular matrix, B, may be found as follows.

(1) Set $b_{rc} = 0$ wherever c exceeds r.

(2) Use equation (4-30) to find b_{11}.

(3) Use equation (4-31) to find $b_{21}, b_{31}, \ldots, b_{m1}$.

(4) Use equation (4-32) or (4-34) to find b_{22}.

(5) Use equation (4-33) to find $b_{32}, b_{42}, \ldots b_{m2}$.

(6) Use equation (4-34) to find b_{33}.

(7) Use equation (4-33) . . . .

4.4 Statement of the Specific Solutions

The covariance matrix for $\underline{N(n)}$ for mode 1 is given in equation (4-10). Samples with the statistics of $\underline{N(n)}$ could be generated using only four scalar, zero-mean, unity-variance samples per vector sample because the covariance matrix has only four nonzero rows; for conceptual clarity and algebraic convenience, the terms on the right-hand side of equation (4-10) were treated separately.

For mode 1,

$$\underline{N(n)} = \sqrt{h} \left\{ (E_{11} + E_{22}) \alpha \sigma_2 \begin{bmatrix} \frac{h}{\sqrt{3}} & 0 \\ \frac{\sqrt{3}}{2} & \frac{1}{2} \end{bmatrix} \begin{bmatrix} z_1(n) \\ z_2(n) \end{bmatrix} \right.$$

$$+ (E_{11} + E_{42}) \sigma_4 \begin{bmatrix} \frac{h}{\sqrt{3}} & 0 \\ \frac{-\sqrt{3}}{2} & \frac{1}{2} \end{bmatrix} \begin{bmatrix} z_3(n) \\ z_4(n) \end{bmatrix}$$

$$+ (E_{11} + E_{22} + E_{33})\,\sigma_5 \begin{bmatrix} \frac{\alpha h^2}{2\sqrt{5}} & 0 & 0 \\ \frac{\sqrt{5}}{2}\alpha h & \frac{\alpha h}{4\sqrt{3}} & 0 \\ \frac{\sqrt{5}}{3}\alpha & \frac{\alpha}{\sqrt{3}} & \frac{\sqrt{9-8\alpha^2}}{3} \end{bmatrix}$$

$$\left.\begin{bmatrix} z_5(n) \\ z_6(n) \\ z_7(n) \end{bmatrix}\right\} \qquad (4\text{-}35)$$

For mode 2,

$$\underline{N(n)} = \sqrt{h}\,(E_{11} + E_{42})\,\sigma_4 \begin{bmatrix} \frac{h}{\sqrt{3}} & 0 \\ \frac{-\sqrt{3}}{2} & \frac{1}{2} \end{bmatrix} \begin{bmatrix} z_1(n) \\ z_2(n) \end{bmatrix} \qquad (4\text{-}36)$$

For mode 3,

$\underline{N(n)}$ = (same as for mode 1 except b_{31} and b_{32} have negative signs in the third triangular matrix) (4-37)

4.5 Comments Concerning Implementation of the Technique

A computer subroutine was written which generates uniform random numbers and sums twelve of these to construct approximately normally distributed, zero-mean, unity-variance, random samples. The particular solutions defined by equations (4-35), (4-36), and (4-37) are added to the homogeneous solutions defined in Chapter 3.

The switching time, t_{n+1}, is a function of the state variables, so that even when it can be stated as an explicit function of $\underline{X(t_n^+)}$, the noise $\underline{N(n)}$ can cause the deterministically predicted value to be in

error. The only case in which noise affects the switching time is in seeking the time at which the velocity reaches zero. Using the Newton-Raphson method, the original guess, g_o, for t_{n+1}, and successive guesses are adjusted essentially as indicated in equation (4-38).

$$g_{i+1} = g_i - \frac{\text{final velocity } (g_i)}{\text{final acceleration } (g_i)} \tag{4-38}$$

In order to avoid bias by rejecting samples in non-random manner, the values of the stochastic vectors, $\underline{Z(n)}$, are held constant during the convergence process. This not only assures that $\underline{N(n)}$ will have the precomputed statistics but also makes convergence of the iterative procedure possible. The process is automatically terminated as soon as the error becomes negligible. The process is usually terminated at the end of the third iteration. It is necessary to switch u(t) to zero at the instant that the torque-motor current decays to zero. The time at which u(t) should be switched to zero can be stated explicitly and solved deterministically. This switching time is always computed first and used as the first guess in equation (4-38). If the first correction computed by equation (4-38) is positive, then the switching of u(t) to zero occurs before the velocity decreases to zero. If the first correction is negative, then the velocity decreases to zero first. In either case, the computer is programmed to make the appropriate decisions and update the state vector from switching point to switching point. Finally, when the prespecified sampling

time precedes any future switching times, that sampling time is treated like a switching point and the plant is updated to that sampling time.

The multimode-linearization equations are considerably harder to program for a computer than the numerical-integration equations; however, the resulting gains in speed and accuracy make the extra effort worthwhile even for certain linear problems.

CHAPTER 5

SOLUTION OF A MULTIMODE-IDENTIFICATION PROBLEM BY USING MODE ESTIMATORS, PARTITIONED AND MODIFIED KALMAN FILTERS, AND BOUNDARY-CONDITION MATCHING

5.1 Introduction

The purpose of the identification process is to estimate the values of the elements of the plant state vector with sufficient accuracy to enable the controller to adequately predict the response of the plant to various appropriate control actions. Unknown plant parameters such as stiction and coulomb friction are also considered as plant-state-vector elements in the identification process. There are many applications of the Kalman-filtering equations to plant-parameter identification in current literature; however, the plants are generally assumed to be linear. Detchmendy and Sridhar have done some work on the estimation of states and parameters in noisy nonlinear systems; however, the systems which they studied were linear in the small (15). That is, the equations of the plants they studied had continuous first and second derivatives. When the assumption of linearity is made, the Detchmendy-Sridhar equations can be reduced to the same form as the Kalman equations and equated term by term; therefore, the Detchmendy-Sridhar equations may be considered to be a generalization of the Kalman equations for

application to nonlinear systems which are linear in the small. The plant equations which are being considered here have abrupt discontinuities with infinite derivatives at the discontinuous points. The only applicable reference to discontinuous-plant equations which was found in the search of modern control literature was the previously mentioned paper by Witsenhausen.

In this chapter, the Kalman-filtering technique is applied to a nonlinear plant with abrupt discontinuities. The same multimode-linearization techniques that were developed in Chapters 3 and 4 are applied to the Kalman-filtering equations. The general principles of the multimode-Kalman-filtering technique are described in the next section, and the specific application of this technique to the plant presently being studied is discussed in the remainder of this chapter.

5.2 General Principles of Multimode-Kalman Filtering

The Kalman-filtering equations were derived under the assumption that the errors in estimating the state vector are linearly related to expected value of the difference between the predicted value and the actual value of some scalar or vector observation. For brevity, the actual observed value minus the predicted observation value is commonly referred to as the "observation residual." When the relationships between the state-vector errors and observation residuals are linear and known, Kalman filtering is the optimum estimation technique (assuming that the noise and errors are normally

independently distributed). When the relationships are mildly nonlinear and the partial derivatives of the observation residuals with respect to the state vector are available, then Detchmendy and Sridhar have shown that their filtering process yields estimates which converge to the correct values; however, no claim of optimality was or could be made. The Detchmendy-Sridhar filter can not be used if the partial derivatives of the observation residual with respect to the state vector are unavailable. When multimode linearization is used, some of the partials are available and some are not. Examples will be given later. For convenience, the state vector for the system can be factored into three parts. The first part is deterministic and can be predicted accurately without any need for filtering. The second part is linearly related to the observation residuals (for a certain mode or certain modes) and can be estimated using the standard-Kalman-filtering equations (for that mode or those modes). The third part is nonlinearly related to the observation residuals, but theoretical study indicated and simulation proved that it can be successfully identified by making the following four modifications to the standard-Kalman-filtering equations.

1. The observations are predicted by using the nonlinear plant model in the controller rather than by linear equations. This is similar to the Detchmendy-Sridhar technique.

2. The matrix relating the observations to the state vector is replaced by a matrix of quasipartials (first-order partial differences). These are obtained by running the plant model in the controller faster than real time, varying one parameter at a time, and dividing the change in the predictions by the change in the parameters.
3. The corrections to the state vector are applied with full weighting, but the reductions to the covariance matrix are multiplied by some empirically determined weighting factor, such as 0.5, in order to compensate for the fact that the corrections are inaccurate because of the nonlinearities.
4. In certain cases, it is helpful or even necessary to add certain nonlinear constraints to the corrections because of the nonlinearities in the plant. No rules have been formulated yet to aid in adding these constraints. At present, the constraints are determined by the use of physical insight, logic, and experience.

This modified-Kalman-filtering technique is not optimal, but it does produce estimates which converge to the true values and, in the simulation, the estimates converged quite rapidly.

The state-vector estimates and covariance matrices in the Kalman equations are projected forward in time using the multimode-linearization techniques developed in Chapters 3 and 4. The system equations and filtering equations are partitioned into the same modes. Although the multimode-linearization technique causes the system equations to become piecewise linear, it does not necessarily linearize the filter equations. One source of nonlinearity in the filtering equations is the fact that the plant mode is generally one of the parameters which must be estimated; hence, the filter must decide which set of linear equations to use at any given time. Another reason for the nonlinearity is that errors in predicting the observations in one mode are often nonlinear functions of state-vector-estimation errors made in some previous mode. Approximate solutions to both of these problems have been found for the specific system being studied. It would not be a trivial task to find a general solution or set of solutions.

The estimation of the system mode becomes an exceedingly complex problem if an optimal solution is sought. If sufficient a priori knowledge is available concerning the system equations, statistics, and cost functions, then the use of a Bayesian strategy would be indicated (16, p. 43). Because of constraints in computer size and speed and the difficulty of computing probability distribution functions for nonlinear systems, it is generally not feasible to use a Bayesian strategy for estimating the plant mode. One of the difficulties in attempting to determine an optimal strategy is the problem of assigning

numbers to the cost of using an observation with the wrong set of mode equations in an attempt to improve the estimate of the state vector. Many observations used with the correct mode equations are usually required to offset the effect of a single observation which was improperly used. The situation will vary considerably depending upon the nature of the nonlinearities, and in some cases the problem will have a simple solution. One scheme which is applicable to a large number of cases is to have as many Kalman filters as the system has modes and to try the observation in all of the filters simultaneously. The filter with the smallest observation residual or smallest weighted observation residual would be selected as the "best estimator." The "best estimator" would be used to update the estimated system-state vector and then all of the other filters would be reset to agree with the "best estimator." The strategy which was used for mode estimation in the simulation was to determine the confidence level for each mode estimate and to ignore observations when the probability of error in estimating the mode was greater than a preset empirical constant. The strategy did not require much computer space or time and gave satisfactory results. Once the starting transients had decayed, all observations were used because the filter was able to predict the mode-switching times quite accurately.

A large amount of theoretical work remains to be done in the development and optimization of multimode-filtering techniques; however, sufficient knowledge is already available for obtaining

useful results in certain applications. The identification of the values of the parameters in the plant defined in Chapter 2 is one such application. The remainder of this chapter describes the filtering strategy which was used for that identification process.

5.3 The Specific Multimode Kalman Filter Used in the Simulation

The function of the multimode Kalman filter is to identify the values of the plant parameters sufficiently well to enable the controller to adequately predict the response of the plant to various appropriate control actions. To accomplish this, it is only necessary to apply corrections to four estimated parameters: $x_1(t)$, $x_4(t)$, k_s, and k_c. It is not necessary to adjust the estimate of the output shaft velocity, $x_2(t)$, because the velocity estimate is set to zero every time the controller model of the plant enters the passive mode (mode 2). No observations are available when the velocity is nonzero; because, during normal operation, the corrective actions are applied immediately after the receipt of a sampling pulse from the error sensor, and these actions are completed, with the velocity back at zero again, before the receipt of the next pulse. For this reason, no provision is made for using observations taken while the system is in mode 1 or mode 3. There is no need to adjust the estimates of torque-motor torque, $x_3(t)$, or the control effort, $u(t)$, because the control effort is directly observable by the controller and $x_3(t)$ is a noise-free deterministic function of $u(t)$. Since the main concern in

the filter study was the starting transients, the simulation runs were all less than 100 seconds in duration. Over that period of time, the value of x_5 was relatively constant so that it could not be separated from the values of $\bar{k}_s$ and $\bar{k}_c$ by the filter. Since the separation was impossible, it was not attempted. The estimate of k_s estimates the sum of $\bar{k}_s$ plus x_5. The estimate of k_c estimates the sum of $\bar{k}_c$ plus x_5. The addition of a separate estimate for x_5 in the filtering equations would be trivially simple from a theoretical point of view.

A large saving in computer programming was obtained by partitioning the four-element system-error-state vector into two parts of two elements each. When the confidence level for the estimate that the system is in mode 2 has risen to approximately 0.9987, then the sampled-data measurements, y(n), of the system error, $x_1(t)$, are accepted and used for improving the estimates of $x_1(t)$ and $x_4(t)$. Since x_2 is constant and equal to zero in mode 2, it is obvious from inspection of figure (2-1), that the estimates of $x_1(t)$ and $x_4(t)$ are sufficient statistics for predicting the observations, y(n), when the system is in mode 2. In mode 2, the relationships between predicted observations and the estimates of $x_1(t)$ and $x_4(t)$ are linear and the observations are discrete, so the standard-discrete-Kalman-filtering equations are used for that portion of the estimation process (17).

The task of improving the estimates of k_s and k_c is not quite so simple as that of estimating x_1 and x_4. If the estimates of k_s and k_c are in error when the controller plant model is in mode 1 or mode 3,

then the controller will predict $x_1(t)$ incorrectly and will also switch into mode 2 at the wrong time so that the initial value for $x_1(t)$ in mode 2 will be in error by some nonlinear function of the nominal values of all of the parameters in the preceding mode interacting with the errors in estimating k_s and k_c. Clearly, the errors in estimating k_s, k_c, and $x_1(t)$ are correlated. If the correlations were linear and known, a four-element error-state vector and conventional Kalman filtering would solve the estimation problem. In this particular nonlinear problem, the computations are simplified and the nonlinear constraints are more easily added when the linear and nonlinear estimation processes are separated. The statistics used for coupling the two estimation processes are the means and the variances of the estimated shaft motions, Δc, which occur during the active phases (mode 1 or mode 3) of the control cycles in response to commanded corrective actions. If the errors of the estimates were normally distributed, then the means and variances of the Δc estimation errors would be "sufficient statistics" for the estimation process.

Suppose that the selected corrective action is to apply control effort, u_{max}, for a period of time, Δt_u. By applying this control effort to the plant model in the controller, it is predicted that this corrective action will cause the output shaft to move by an angle, Δc_p. The error in predicting Δc is not normally distributed but usually the distribution is close to normal. The error in estimating Δc is estimated with the aid of the quasipartials which were discussed earlier.

$$E\left[\Delta c_p - \Delta c\right] \doteq \mathrm{VAR}\left[\Delta c_p\right] \doteq H_b P_b H_b', \quad \Delta c \neq 0 \qquad (5\text{-}1)$$

$$H_b' \triangleq \begin{bmatrix} (\text{quasipartial of } \Delta c_p \text{ with respect to } \hat{k}_c) \\ (\text{quasipartial of } \Delta c_p \text{ with respect to } \hat{k}_s) \end{bmatrix}_{\Delta t_u = \text{constant}} \qquad (5\text{-}2)$$

$$\hat{k}_c \triangleq \text{the estimate of } k_c \qquad (5\text{-}3)$$

$$\hat{k}_s \triangleq \text{the estimate of } k_s \qquad (5\text{-}4)$$

$$P_b = \begin{bmatrix} E\left[(\hat{k}_c - k_c)^2\right] & E\left[(\hat{k}_c - k_c)(\hat{k}_s - k_s)\right] \\ E\left[(\hat{k}_c - k_c)(\hat{k}_s - k_s)\right] & E\left[(\hat{k}_s - k_s)^2\right] \end{bmatrix} \qquad (5\text{-}5)$$

The means and variances of the Δc predictions are used to reset the estimates of $x_1(t)$ and the covariance matrix for estimation error in the mode 2 linear Kalman-filter equations. An additional variance term was computed and added to equation (5-1) to account for the large estimation errors which would occur if the output shaft did not move at all. As the control-effort-application period, Δt_u, is gradually decreased, the magnitude of the output motion, Δc, will gradually decrease to a minimum value, Δc_{min}, and then drop abruptly to zero. When there are stochastic factors present, the value of Δc_{min} and the corresponding minimum useful control-effort-application period, $\Delta t_{u,\,min}$, are not deterministically predictable. Values of Δt_u are never chosen smaller than $\Delta t_{u,\,min}$ by intent; however, during the first few seconds of system operation, when the estimate of k_s is still fairly inaccurate, such errors are common. The error in estimating Δc is not distributed normally; however, Detchmendy and Sridhar showed that the convergence of

the filtering process does not depend upon the distributions being normal or even upon having the correct estimates for the variances. The variance approximated by equation (5-1) is the variance of Δc_p estimated under the condition that $\Delta c \neq 0$. For convenience, it is referred to simply as "the conditional variance of Δc_p." When the conditional restriction is removed, the variance is estimated by the following approximation and called "the total variance of Δc_p."

Define

$$\Delta c_{p,\,cond} \triangleq \text{prediction of } \Delta c \text{ given } \Delta c \neq 0 \qquad (5\text{-}6)$$

$$\Delta c_{p,\,total} \triangleq \Delta c_{p,\,cond} \ \mathrm{Prob}(\Delta c \neq 0) \qquad (5\text{-}7)$$

Then,

$$E\left[(\Delta c_{p,\,total} - \Delta c)^2\right] \doteq H_b P_b H_b' + (\Delta c_{p,\,cond})^2 \mathrm{Prob}(\Delta c = 0)\ \mathrm{Prob}(\Delta c \neq 0) \qquad (5\text{-}8)$$

$$E\left[(\Delta c_{p,\,cond} - \Delta c)^2\right] \doteq H_b P_b H_b' + (\Delta c_{p,\,cond})^2 \mathrm{Prob}(\Delta c = 0) \qquad (5\text{-}9)$$

$$E\left[(\Delta c_{p,\,cond} - \Delta c)^2\right]_{cond} \doteq H_b P_b H_b' \qquad (5\text{-}10)$$

If the objective is to minimize the error in estimating $x_1(t)$ and $x_2(t)$ for all cycles, then equations (5-7) and (5-8) should be used for resetting the mode 2 filter. On the other hand, if the object is to obtain the best estimates possible for correcting $\hat{k}_s$ and $\hat{k}_c$, then equations (5-6) and (5-9) should be used because $\hat{k}_s$ and $\hat{k}_c$ are not updated in any particular controller cycle unless the confidence level for the hypothesis that $\Delta c \neq 0$ is equal to or greater than approximately 0.98. Equations (5-6) and (5-9) were chosen because errors

in estimating k_s and k_c would degrade the system performance more severely and for longer periods of time than corresponding errors in $\hat{x}_1(t)$ and $\hat{x}_4(t)$.

The following method is used for estimating the time, t_{max}, at which the confidence level becomes 0.9987 for the assumption that the system has returned to the passive mode (mode 2).

$$t_{max} \triangleq t_{nominal} + 3\sqrt{H_{tb}\, P_b\, H'_{tb}} \tag{5-11}$$

$$H'_{tb} \triangleq \begin{bmatrix} (\text{quasipartial of } t_{nominal} \text{ with respect to } k_s) \\ (\text{quasipartial of } t_{nominal} \text{ with respect to } k_c) \end{bmatrix}_{t_u = \text{const.}} \tag{5-12}$$

The values of H_{bt} are found as a by-product of determining those of H_b; the only extra computer operations required are two division and two storage operations.

The observations in mode 2 are used to improve the estimates of $x_1(t)$ and $x_4(t)$. At the end of mode 2, $\hat{x}_1(t)$ and $\hat{x}_4(t)$ are used to construct an estimate, Δc_m, which is an indirect measurement of the output motion, Δc, which occurred as a result of the last corrective action. Suppose that $\hat{x}_1(t_a)$ is the estimate of $x_1(t)$ which was made just before the last corrective action and that $\hat{x}_1(t_b)$ and $\hat{x}_4(t_b)$ are the estimates made just prior to the next corrective action. Since $x_4(t)$ is effectively constant for such short time periods, the shaft motion, Δc, may be estimated as follows.

$$\Delta c_e = \hat{x}_1(t_b) - \hat{x}_1(t_a) + \hat{x}_4(t_b)\,(t_b - t_a) \tag{5-13}$$

$$\text{VAR}\left[\Delta c_e\right] \doteq \text{VAR}\left[\hat{x}_1(t_b)\right] + \text{VAR}\left[\hat{x}_1(t_a)\right] + 2\,\text{COV}\left[\hat{x}_1(t_b),\, \hat{x}_1(t_a)\right](t_b - t_a) + \text{VAR}\left[\hat{x}_4(t_b)\right](t_a - t_b)^2 \tag{5-14}$$

Using the parameters defined above and continuing to follow the notation of R. C. K. Lee, the modified-Kalman-filtering technique for identifying k_s and k_c may be outlined using four matrix equations (17).

$$P_{n+1|n} = \bar{\Phi} P_{n|n} \bar{\Phi} + \mathrm{COV}\left[\underline{N(n)}\right] \tag{5-15}$$

The value of COV $\left[\underline{N(n)}\right]$ is given by equation (4-10) or (4-12).

$$K_{n+1} = P_{n+1|n} H_b' \left[H_b P_{n+1|n} H_b' + \mathrm{VAR}\left[\Delta c_e\right]\right]^{-1} \tag{5-16}$$

$$\begin{bmatrix} \hat{k}_c \\ \hat{k}_s \end{bmatrix}_{n+1} = \bar{\Phi} \begin{bmatrix} \hat{k}_c \\ \hat{k}_s \end{bmatrix}_n + K_{n+1} \left[\Delta c_e - \Delta c_{p,\,\mathrm{cond}}\right] \tag{5-17}$$

$$P_{n+1|n+1} = \left[I - a K_{n+1} H_b\right] P_{n+1|n} \tag{5-18}$$

The scalar, a, in equation (5-18) would be equal to unity for ordinary-linear Kalman filtering; however, the nonlinear filtering equations make use of certain approximations so that the covariance matrix of estimation error, $P_{n+1|n+1}$ is not reduced as much by the $(n+1)^{th}$ correction as it would have been if the correction had been exactly optimum. Empirically, it was found that when the value of the coefficient, a, was set equal to 0.5 that the filter operated very satisfactorily when started with initial errors which were in error by factors of two. As the errors become smaller, the filtering equations become more accurate; therefore, the coefficient, a, should probably be made to vary as some function of the magnitude of the observation residuals.

If no nonlinear constraints are added to the estimation equations, it is conceivable that k_s could be "corrected" to a magnitude

larger than the maximum torque which was applied during the cycle in which the "correction" occurs. Such a "correction" would be fallacious, because it has already been decided that motion occurred but motion can not occur if the magnitude of k_s exceeds that of the maximum applied torque. If any such fallacious "corrections" occur, they are detected by an inequality test in the computer, the magnitude of the quasipartial for k_s is reduced by an appropriate amount and the estimates are recomputed exactly as before except for the adjustment of H_b. This corrective procedure may be repeated several times. There are two reasons why readjusting the quasipartial for k_s is superior to merely operating directly on the estimate for k_s. First, it gives a better correction for k_c. Second, it produces a more realistic correction to the covariance matrix. Another nonlinear constraint was added to prevent k_s from being reduced below the magnitude of k_c.

If large initial errors are expected during the starting period, constraints should be added to limit the magnitudes of the individual corrections because the linear approximations are inaccurate for large increments. Constraints must not be added indiscriminately or the covariance matrix, P, will become inaccurate. If the covariance matrix becomes inaccurate, the efficiency of the filter deteriorates. One way to reduce the gain without invalidating the covariance matrix is to insert a fictitiously large number into equation (5-16) in the place of $\mathrm{VAR}\left[\Delta c_e\right]$.

5.4 Conclusions Concerning Multimode Kalman Filtering

Although the techniques for nonlinear-multimode Kalman filtering are not as simple to apply as those of ordinary Kalman filtering, they are still tractable. When used along with multimode linearization, the multimode-filtering technique becomes another method for estimating state vectors and identifying parameters in nonlinear systems. A vast amount of theoretical exploration of the technique remains to be done; however, it is already sufficiently well developed to have immediate practical applications. The nonlinear-multimode Kalman filter described in the preceding section worked the first time it was tried. The only thing that was changed thereafter was the value of the coefficient, a, in equation (5-18).

CHAPTER 6

DEFINING, EVALUATING, AND MINIMIZING THE COST FUNCTION

6.1 Defining, Evaluating, and Minimizing the Cost Function Given the Control-Effort Duration, Δt_u

It is necessary to define a cost function in order to establish a basis of comparison between various control strategies. If there were no constraint on power, the solnic system would make corrections so frequently that the resulting control-effort signals would look very similar to square-wave dither except that the switching times would be precisely governed by the controller rather than synchronized in a relatively inflexible manner to the waveform of an external dither oscillator. The study of solnic systems under such operating conditions would be of great theoretical interest; however, the application motivating this study is the design of gimbal-control servomechanisms for inertial-guidance platforms. For such applications, the expenditure of large amounts of energy is objectionable, not only in that it wastes energy, but also because it creates thermal gradients which degrade the performance of the inertial components. In order to progress toward the original objective, it was necessary to assign a cost to control effort as well as to control error. The cost function was defined as the sum of two terms: the first term represents the

cost of positional error and the second represents the cost of control effort.

The solnic system applies corrections to the plant on a cyclic basis and changes strategy from cycle to cycle; therefore, it is desirable to define the cost function on a single-cycle basis. First, it is necessary to define what is meant by the term "a cycle." In section 3.2, it was explained that the optimum control strategy for controlling the plant under consideration here is to switch the control effort, u(t), to plus or minus the maximum allowable magnitude, u_{max}, and after some precomputed time switch it back to zero, allowing the arc-suppression diodes to apply reverse voltage until the torque-motor current decays to zero. The nth cycle will be defined as the period of time between the instant at which u(t) is switched from zero to the magnitude of u_{max} for the nth time and the instant at which it is so switched for the $(n+1)^{th}$ time. For the sake of completeness, the definition of the cycle period will be extended to include the former instant and exclude the latter.

During any control cycle, there are just three parameters of the control variable which the controller may adjust: the switch-on time, the sign of u(t), and the switch-off time. The sign of the corrective action is obviously chosen so as to drive the value of $x_1(t)$ toward zero. Before a control action is taken, a prediction, Δc_p, is made of the amount that the output shaft will be moved by that corrective action. If a series of identical corrections are to be made,

then in order to minimize the positional errors it is necessary to control the timing of the corrections so that $x_1(t)$ will have an average value of zero. This may be accomplished by the very simple procedure of waiting until the magnitude of the error becomes half as large as that of Δc_p before initiating the corrective motion. When the system is operated in accordance with this strategy, the peak errors will be approximately half as large as the magnitude of the step corrections. If the solnic system estimators are inaccurate, the peak errors will be larger than half the magnitude of the step corrections, Δc; however, the difference was negligible after the first 20 seconds for the cases simulated on the computer. Even when identification errors are significant, the above strategy minimizes the expected value of the errors. Now that the optimum strategies have been formulated for the direction and timing of the control-effort applications, the only unspecified parameter remaining is the control-effort duration, Δt_u. The optimization of Δt_u is discussed in section 6.2. Before considering the optimization of Δt_u, the cost function will be defined in terms of equations which can be evaluated within the controller using the estimated values of the plant variables and parameters.

To keep the controller operation optimal in spite of stochastic variations of the environmental and plant parameters, the controller computes the cost of various control strategies and changes its strategy accordingly. The best data available to the controller concerning

the state of the system and the environment is the information from the estimators described in the preceding chapter; therefore, the cost function is defined in terms of those estimated parameters. Since the parameter estimates are obtained by filtering over a relatively long period of time compared with one or a dozen control-cycle periods, the cost estimates are far more accurate than they would be if the costs were estimated on the basis of direct measurements taken only during the period when the system was operated in accord with the strategy in question.

From previous discussions, it is obvious that when noise is neglected the best estimate for the magnitude of the peak-to-peak error is equal to the absolute value of Δc_p. The exact effect of various noise sources on the cost of control is difficult to determine because of the nonlinearity of the problem; however, the following equation gives a relatively accurate estimate of the peak-to-peak error cost, C_1, which is easy to compute.

$$C_1 \doteq \sqrt{(\Delta c_p)^2 + VAR(\Delta c_p) + VAR[x_1(t)]} \qquad (6\text{-}1)$$

The variances in the above equation were negligible and were neglected for the examples run in the simulation. From log-log plots of C_1 versus the control variable Δt_u, it was noted that the magnitude of C_1 increases proportionally with the sixth, fifth, fourth, and third powers of Δt_u over the range of interest. The larger the magnitude of Δt_u became the smaller the exponent became.

In establishing a cost function for control effort, it was decided that the average current from the power supply should be minimized. The average current is estimated by computing the number of coulombs which flow from the battery during the control-effort-application period, Δt_u, and dividing this number by the duration of the control cycle measured in seconds. The first number may be readily computed as follows since the supply voltage, E, and the torque-motor resistance, R, are assumed to be known.

$$Q = \frac{V}{R}\left[\mathrm{EXP}(-\beta_3 \Delta t_u) - 1 + \beta_3 \Delta t_u\right] \qquad (6\text{-}2)$$

Assuming that the system is caused to cycle repetitively with the same strategy, then the duration of the control cycle, T, may be estimated as follows.

$$T \doteq \frac{|\Delta c_p|}{\hat{x}_4} \qquad (6\text{-}3)$$

Defining a constant, a_c, which is used to express the ratio of positional error cost to power cost, the cost function for control effort, C_2, and the total cost, J, may be computed as shown in equations (6-4) and (6-5).

$$C_2 \doteq a_c \left(\frac{Q}{T}\right) \qquad (6\text{-}4)$$

$$J = C_1 + C_2 \qquad (6\text{-}5)$$

The value of the coefficient a_c was selected so that, if the solnic system were able to operate optimally with respect to that cost function, then it would be operating with peak errors about an order of magnitude smaller than the classical limit stated in equation (2-6).

6.2 Optimizing the Control-Effort Duration, Δt_u

If the estimated values of all of the system variables and parameters were correct, then the optimum operating strategy could be determined inside of the controller without operating the system. If, however, the control strategy were optimized internally without experimentation, then only a single control strategy would be used. Using only a single strategy, it would be impossible to separate the errors in estimating k_s from those in estimating k_c; therefore, these two errors would become highly correlated and both estimates would be inaccurate. Without accurate estimates of k_s and k_c, the cost functions could not be estimated accurately for alternate strategies; and therefore, the optimization process would be inaccurate. The control strategy must be varied sufficiently to avoid singularity in the identification process or the optimum strategy will not be correctly identified. Varying the strategy away from the optimum point in order to improve identification, increases the cost of control. This is the identification-singularity versus cost-nonoptimality dilemma mentioned in section 1.2.

In order to converge quickly toward the optimum operation point, avoid identification singularities, and follow any changes; the controller in the computer simulation was programmed to vary strategy and reoptimize frequently. It was estimated a priori that a two-to-one variation in the size of the output motion, Δc, would be sufficient to avoid the singularity problem. Provision was made in

the computer program for changing this ratio, but it was never changed. During normal operation, the controller operates for four cycles with Δc about equal to 0.707 times the computed optimal size, four cycles at the optimal size, and four cycles at about 1.414 times the optimal size. After each set of twelve cycles, it computes the cost functions for each size and then recomputes the optimal point. All of the optimization computations and corrections are evaluated and applied in terms of Δt_u because Δc is not directly controllable. Two terms are used to define the three sizes of Δt_u which are used. The computed optimal value of Δt_u is represented by the symbol, $\Delta t_{u,\,opt}$. The symbol $\Delta t_{u,\,inc}$ represents the incremental difference between adjacent sizes of Δt_u.

$$\Delta t_{u,\,small} = \Delta t_{u,\,opt} - \Delta t_{u,\,inc} \tag{6-6}$$

$$\Delta t_{u,\,medium} \triangleq \Delta t_{u,\,opt} \tag{6-7}$$

$$\Delta t_{u,\,large} = \Delta t_{u,\,opt} + \Delta t_{u,\,inc} \tag{6-8}$$

The value of $\Delta t_{u,\,inc}$ is adjusted every twelve cycles as shown below. The coefficient, a_{gain}, was set equal to 0.3 and the coefficient, a_{ratio}, was set equal to two.

$$\Delta t_{u,\,inc}(n+1) = \Delta t_{u,\,inc}(n)\left[1 - a_{gain}\left(\frac{\Delta c_{p,\,large}}{\Delta c_{p,\,small}} - a_{ratio}\right)\right] \tag{6-9}$$

The equation for revising the estimate of $\Delta t_{u,\,opt}$ was derived by plotting the costs versus the duration of Δt_u for the three different sizes, fitting a parabola through the three points, and differentiating

to find the minimum point. Equation (6-10) sets the new value for $\Delta t_{u,\,opt}$ at the minimum point on the parabola (or the maximum point if the cost function is convex upward). Nonlinear constraints were added to limit the change in $\Delta t_{u,\,opt}$ to no larger than $\Delta t_{u,\,inc}$ for any one correction and to make a maximum-size correction in the downward direction when the sampled portion of the cost curve is convex upward. These constraints are needed because the cost curve is highly nonlinear and does have sections which are convex upward.

$$\Delta t_{u,\,opt}(n+1) = \Delta t_{u,\,opt}(n) + \frac{J_{large} - J_{small}}{2(J_{small} + J_{large}) - 4J_{medium}} \Delta t_{u,\,inc}(n) \qquad (6\text{-}10)$$

The subscripts, large, medium, and small, refer to the size of Δt_u used in computing the cost functions. These algorithms were tested directly on the deterministic cost function before the rest of the simulation was completed. The magnitude of the coefficient, a_{gain}, in equation (6-9) was changed from 0.2 to 0.3 to hasten the convergence. No other changes were made. The algorithms converged in all cases as long as the initial value of $\Delta t_{u,\,inc}$ was greater than zero and that of $\Delta t_{u,\,opt}$ was not negative.

CHAPTER 7

THE DIGITAL SIMULATION

7.1 Introduction

The primary objective of the simulation was to determine whether or not the solnic strategy would enable the controller to maintain the positional error of the plant below the minimum error level obtainable using classical, linear, time-invariant control strategies. The simulation program was written in FORTRAN using the multimode-linearization techniques described in Chapters 3 and 4. As a by-product of the prime objective, it was established that the multimode-linearization technique for simulating nonlinear stochastic systems is practical, fast, and accurate. It was also shown that the multimode Kalman filter quickly and accurately identified the unknown parameters of the stochastic, nonlinear plant. The solnic system was shown to identify the optimal strategy and converge to it quickly for a wide range of initial conditions and several cost functions. Once it had definitely been established that the solnic system could consistently maintain the positional error of the plant an order of magnitude smaller than the minimum error level obtainable using classical, linear, time-invariant control strategies; the simulation work was terminated with no effort to find the lowest

obtainable error level. The prime objective and subsidiary objectives had been reached.

7.2 Mechanics of the Simulation

The digital computer program for the simulation was written using a modified version of the FORTRAN II computer language. The instructions were fed directly into an SDS 930 computer from a card reader, and the results were typed out by an on-line printer as quickly as they were computed. The computer program ran faster than the line printer, so it was necessary to curtail type-out considerably when all of the pieces of the program were assembled into a working whole. To facilitate the detection and correction of errors, the program was divided into six major pieces plus two subroutines and the equivalent of a third subroutine. The parts of the program were tested and corrected individually using a large number of print statements to assure that each of the parts was functioning properly. When the program was run as a whole, the type-out was limited to two points and one set of filter statistics per control cycle; even so, the line printer was slower than the computer. Use of the multimode-linearization techniques made it possible to simulate the nonlinear, stochastic plant and the identification and control system for that plant at a speed greater than the line printer could type and with an accuracy limited only by the round-off errors of the computer. The SDS computer words have 23 significant bits plus exponent and sign;

therefore, the round-off noise should be negligible compared with the noise which is generated and introduced intentionally.

The general operation of the computer program can be understood from a study of the highly simplified computer flowchart shown in figure (7-1). The procedure for updating the values of the plant variables is summarized in section 4.5. The filtering techniques are explained and the filtering and estimation equations are defined in section 5.3. The evaluation of the cost functions and the algorithms for adjusting $\Delta t_{u,\,opt}$ and $\Delta t_{u,\,inc}$ are covered in detail in Chapter 6. One thing which has not been mentioned previously, is that the test to see whether or not corrective action is required is an unsymmetrical test.

In section 6.1, it was stated that in order to minimize the peak magnitudes of the errors, the corrective motions should be initiated when the slowly increasing, estimated error, $\hat{x}_1(t)$, reaches half of the magnitude of the estimated size of the correction, Δc_p. That statement defines one limit for the unsymmetrical test to determine whether or not corrective action is required. If the controller predictions are unbiased, then the probability is 0.5 that the magnitude of $x_1(t)$ will be greater than half that of Δc_p at the instant that a randomly chosen corrective motion ceases. It would not be desirable to correct for such an error unless it were unusually large, because the effect of $x_4(t)$ will usually correct for such errors quite rapidly with no expenditure of control effort. Such errors were called overshoot

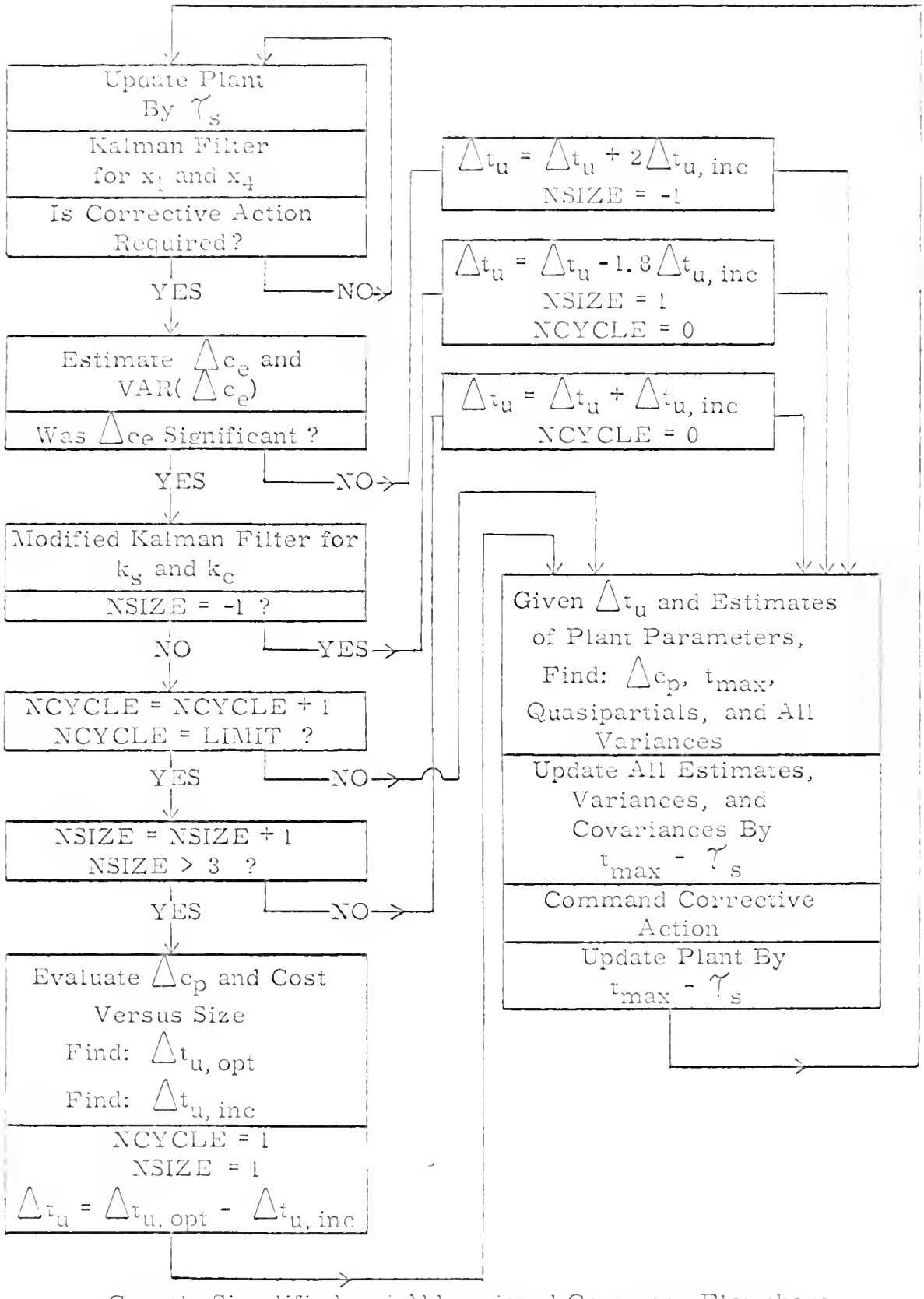

Greatly Simplified and Abbreviated Computer Flowchart
(Stressing Logic for Adjusting Δt_u and NSIZE)

Figure 7-1

errors. The second limit in the unsymmetrical test was set so that overshoot errors are not corrected for unless the magnitude of $\hat{x}_1(t)$ becomes greater than 1.5 times the magnitude of Δc_p. The only time that an overshoot error large enough to exceed the second limit occurred was when the system was starting and the initial estimates for k_s and k_c had been intentionally set at twice the size of the true values.

Although only three sizes of corrections are used for the cost-optimization procedure described in section 6.2, figure (7-1) shows five sizes: -1, 0, 1, 2, and 3. The last three sizes are the three sizes used for cost optimization. The first two sizes, -1 and 0, are normally used only during starting transients when the estimates of the plant parameters and variables are inaccurate and $\Delta t_{u,\,opt}$ and $\Delta t_{u,\,inc}$ not yet properly adjusted. Whenever the magnitude of the estimated value of Δc is less than twice that of its standard deviation, the controller does not use that estimate for updating $\hat{k}_s$ and $\hat{k}_c$; instead, it switches to cycle size -1. When the cycle-size designating symbol, NSIZE, is set to -1, the controller repetitively increases Δt_u, applies corrections to the plant, and tests for significant motion. When significant motion is detected, NSIZE is set to size 0 and Δt_u is decreased; however, it is decreased less than it was increased. Once the value of Δt_u for size 0 has been increased sufficiently to produce significant motion, the system returns to the normal, three-size mode of operation described in Chapter 6. As the filters receive

information, the estimates improve and the variances decrease so that smaller values of Δc_e become significant. The cycle-size incrementing scheme described above is definitely not optimal. However, the scheme was good enough to get the controller started from a wide range of initial conditions. When the starting transients caused by the intentionally erroneous initial estimates decayed, cycle sizes -1 and 0 were no longer used so that the system behaved in the more nearly optimal manner described in Chapter 6.

7.3 Description of a Typical Computer Run

The values of the plant parameters specified in table (2-1) were used for all of the computer simulations. Only the cost ratio, a_c, in equation (6-4), and the initial values of $\hat{k}_s$, $\hat{k}_c$, $\Delta t_{u,\,opt}$, and $\Delta t_{u,\,inc}$ were changed. The initial estimates of $x_1(t)$ and $x_4(t)$ were always set to zero. As long as the cost function remained unchanged, the different simulation runs all converged to the same operating conditions.

For one typical run, the initial estimates of k_s and k_c were set equal to half the magnitudes of the correct values. The value of $\Delta t_{u,\,inc}$ was set four times too large in size. The magnitude of $\Delta t_{u,\,opt}$ was initialized at zero. The minimum obtainable peak error for this plant using a classical, linear, time-invariant controller is given by equation (2-6) as about seven micro-radians. The results for the simulated solnic system are shown in figures

(7-2), (7-3), (7-4), and (7-5). The largest positional error was about 25.7 micro-radians, and it occurred about five seconds after the controller was started. It took the controller about ten seconds to get away from cycle sizes -1 and 0 and begin the first set of three cycle sizes as described in Chapter 6. The first cost-function computation and $\Delta t_{u,\,inc}$ adjustment occurred at 20 seconds. The controller was cycling relatively slowly during the first 20 seconds because it was making large Δc corrections (Δc_{large} = 45 micro-radians). The true value of $x_4(t)$ at 20 seconds was 29.387 micro-radians per second, and the estimated value was 29.376 micro-radians per second. (The estimate for $x_4(t)$ had already converged with less than 1 percent error in the first two seconds.) The estimates for k_s and k_c were 71 and 102 percent of their correct values, respectively.

At 54 seconds, the controller computed the cost functions for the fourteenth time. The estimates for $x_4(t)$ and k_c were about the same as they were at 20 seconds, except that their variances had been reduced. The estimate for k_s had improved greatly because the reduction of the size of the positional corrections, Δc, made the effect of stiction more significant. The estimate for k_s was equal to about 95 percent of its true value. The controller had identified $\Delta t_{u,\,opt}$ to four significant figures, had adjusted the size ratio for the large and small positional corrections to 2.1. The system was operating consistently with peak errors of 0.94, 1.4, and 2.0 micro-radians for the small, medium, and large Δc's, respectively. It is

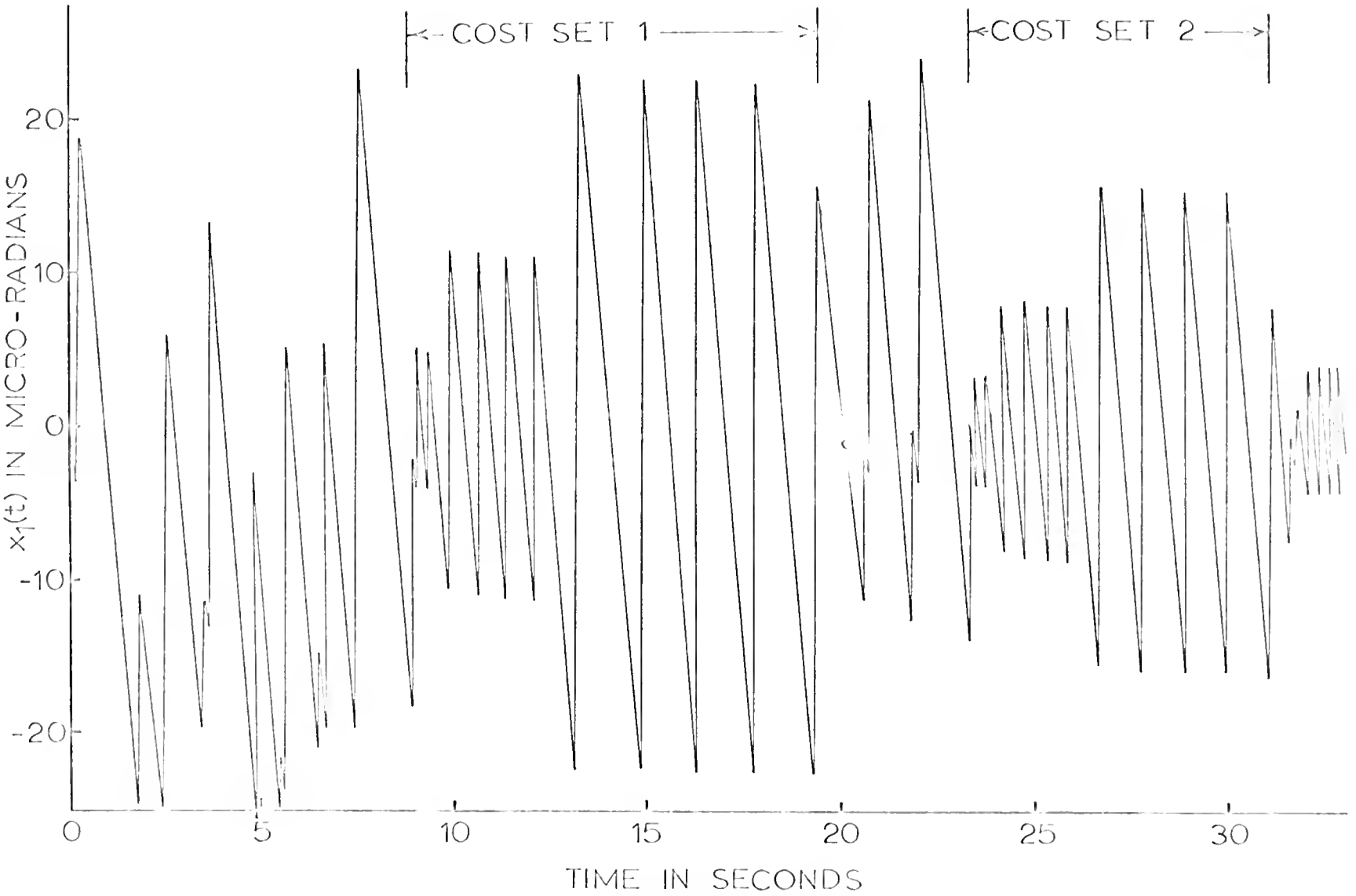

FIGURE 7-2 ERROR VERSUS TIME

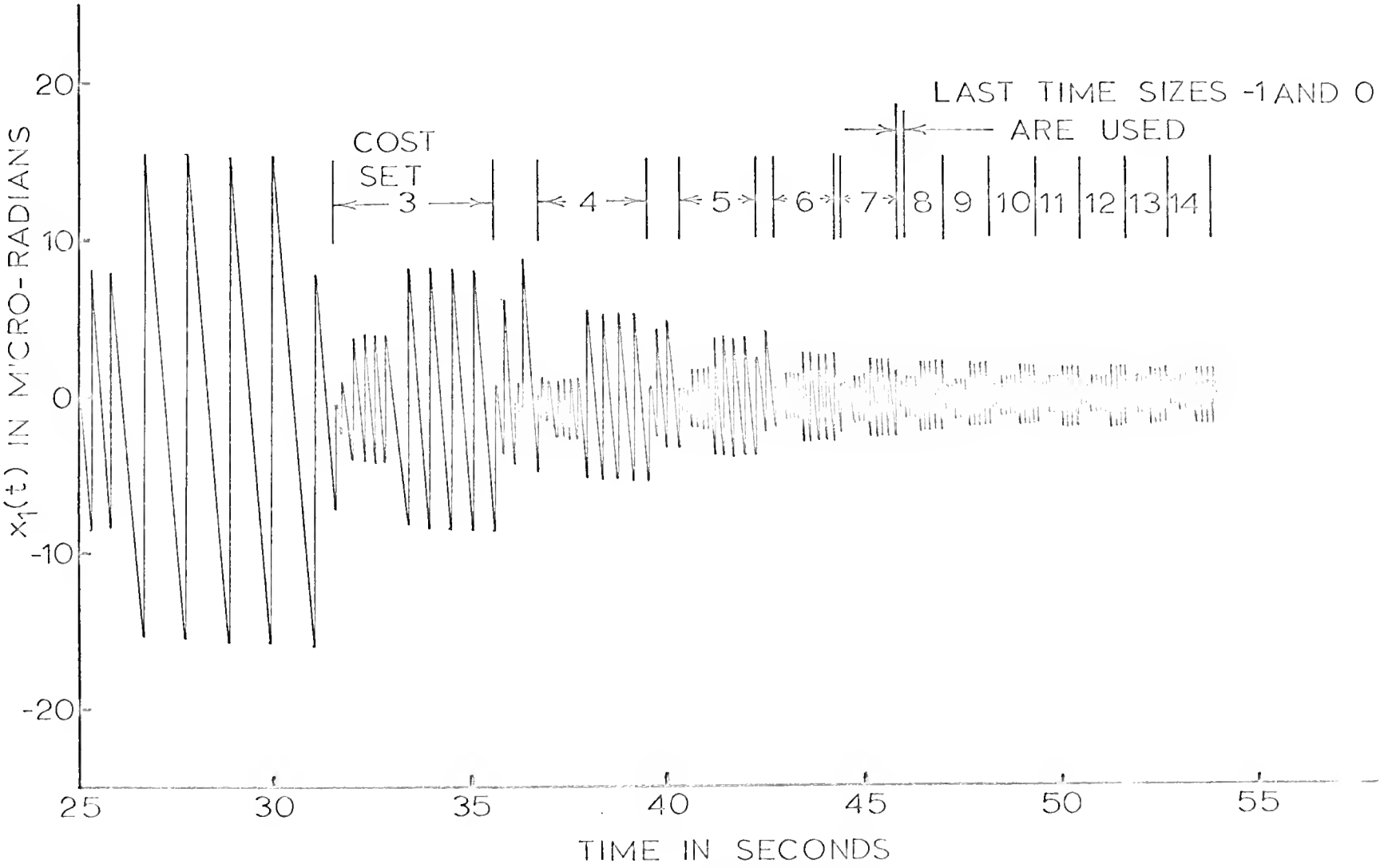

FIGURE 7-3 ERROR VERSUS TIME, CONTINUED

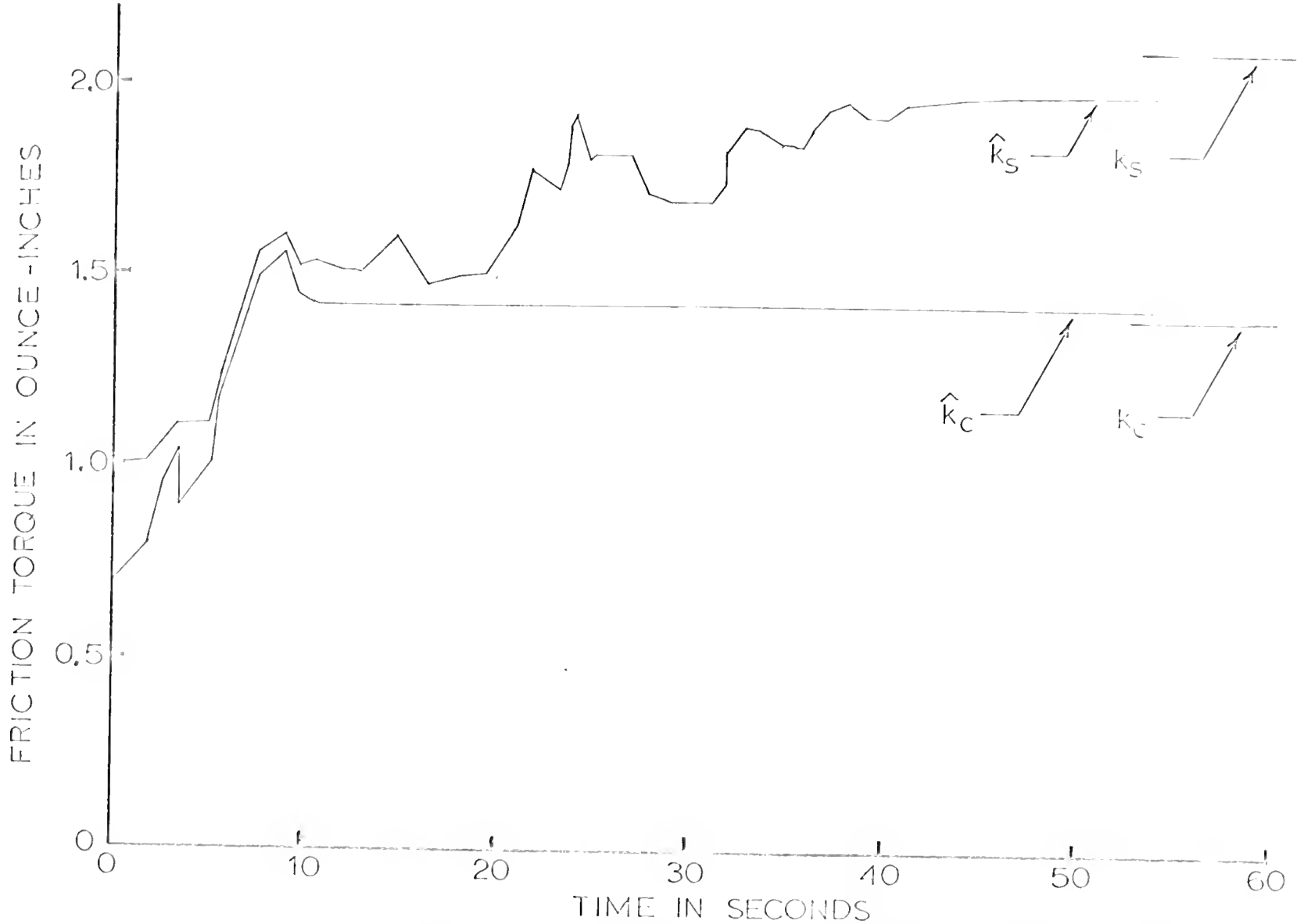

FIGURE 7-4 FRICTION ESTIMATES VERSUS TIME

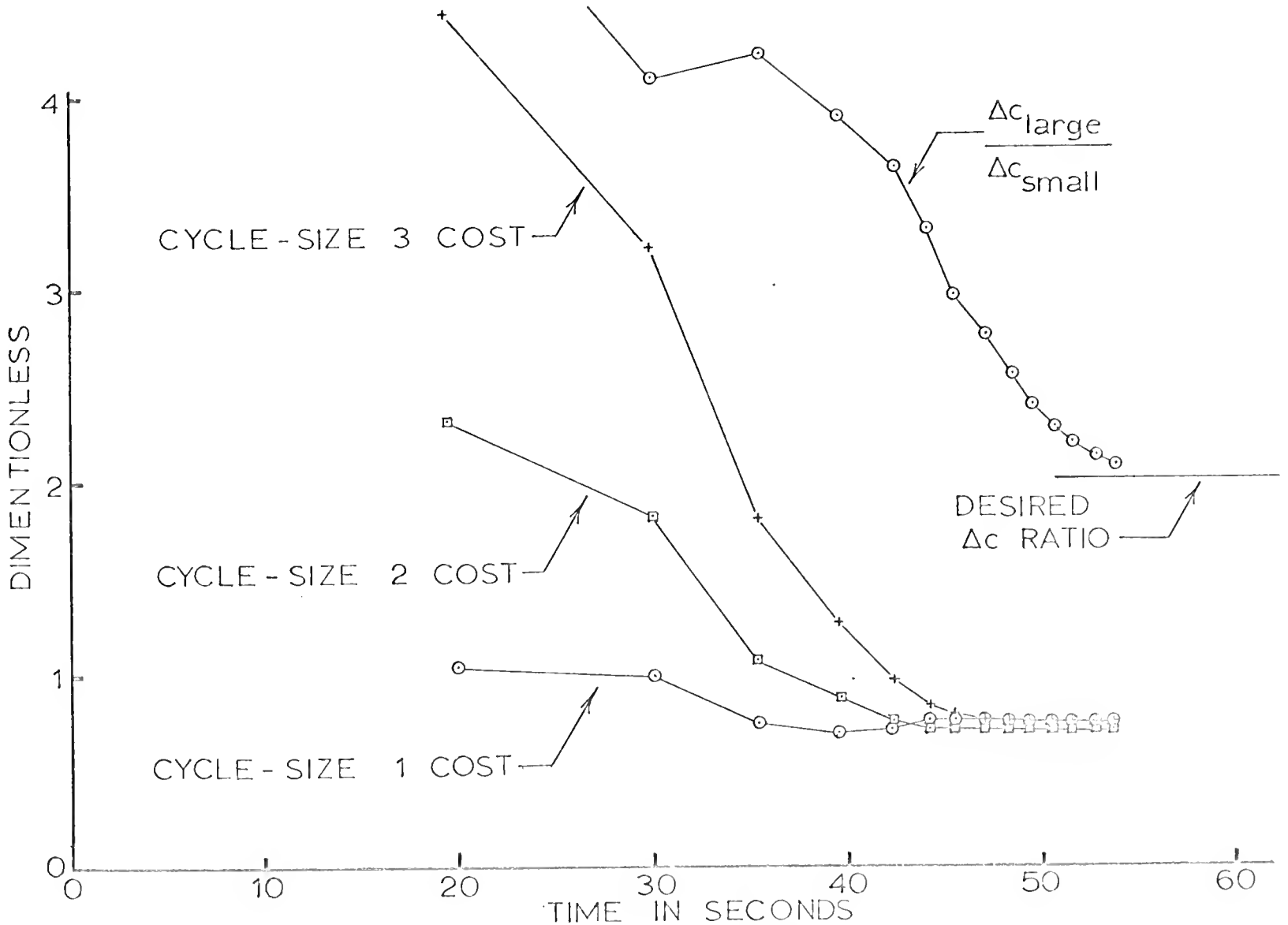

FIGURE 7-5 COST AND Δc RATIO VERSUS TIME

very significant that the errors in estimating k_s and k_c had opposite signs. The correlation between the two estimates was -0.65 according to the covariance matrix in the filter. The two errors were cancelling each other out sufficiently well that the predicted and observed values of the positional corrections, Δc_p and Δc_e, were agreeing with each other consistently to three significant figures for all three sizes. This is a specific illustration of the identification-singularity versus cost-nonoptimality dilemma which was first mentioned in section 1.2.

7.4 Conclusions from the Simulations

The first conclusion reached was that the advantage in simulation speed obtained by using the multimode-linearization techniques rather than numerical integration justified the increased time spent in writing the computer program.

As had been anticipated, the modified-Kalman-filtering equations for estimating the values of k_s and k_c produced better estimates when the magnitude of the coefficient, a, the gain coefficient for the adjustments to the covariance matrix in equation (5-18) was reduced from unity to one half. The cases in which one half was obviously superior to unity were the cases in which the initial estimates of k_s and k_c were intentionally set in error by factors as large as two. When the initial estimates were approximately correct, the magnitude of unity may have been superior, but this was not obvious from the simulation.

From the computer run described in section 7.3, and from other runs made with different cost functions, it was concluded that the solnic strategy enabled the controller to consistently identify the parameters of the nonlinear plant, and that, after a brief learning period, the controller could maintain the peak errors an order of magnitude lower than could be maintained using the classical, time-invariant, linear control strategies. No attempt was made to determine how much lower the error could be reduced by further changes in the cost function. The original objective had been accomplished.

CHAPTER 8

CONCLUSIONS, APPLICATIONS, AND TOPICS FOR FURTHER STUDY

8.1 Conclusions

The plant with the inertial load and nonlinear friction described in Chapter 2 can be controlled at least ten times more accurately by use of a solnic strategy than by use of the most accurate, time-invariant, nonlinear control strategy. At the same time that the solnic system is performing with less error, it is also operating at a lower average power level than the linear, time-invariant system. The ultimate accuracy attainable with the plant defined in Chapter 2 using a solnic strategy has not been determined. The solnic system was able to identify and operate in conformance with the optimum control policy for the cost function stated in equation (6-5); however, in order to avoid singularities in the identification process, nonoptimal policies were also used. That is, to avoid identification singularities, a mixed rather than a pure optimal strategy was used.

The multimode-linearization technique developed in Chapters 3 and 4 for simulation of stochastic, nonlinear systems saved so much computer time that it is worthy of consideration even for much simpler simulations.

The multimode Kalman filter used in conjunction with the multimode-linearization techniques identified the parameters of the highly nonlinear plant quickly and accurately in the presence of noise.

8.2 Applications

The specific solnic system simulated during this study was designed to control the plant defined in Chapter 2. As was pointed out in section 2.4 and elsewhere, real plants are generally far more complicated than the plant which was chosen for the simulation. The specific controller developed in this study does not necessarily have a direct application; however, it did demonstrate that a solnic system can outperform the best classical, linear, time-invariant controller by at least an order of magnitude in accuracy. It was also demonstrated that the solnic system consumed less power. Therefore, the solnic concept should be considered for immediate application to nonlinear systems which can not be controlled adequately using classical techniques.

The multimode-linearization technique for the digital simulation of stochastic, highly nonlinear, differential systems was developed merely as a tool for testing the solnic concept; however, it is directly applicable to many other problems. The speed and accuracy advantages of this technique make it attractive even for much simpler applications. The same multimode-linearization techniques can be used to perform error analyses by applying them to the covariance matrices of system error.

The multimode-Kalman-filter technique has applications in many diversified areas such as coding, game theory, and controls. When using along with the multimode-linearization technique, it provides another means of identifying the parameters of a highly nonlinear plant in the presence of measurement and plant noise.

8.3 Topics for Further Study

No attempt has been made to determine how accurately the specific solnic system described in this study would control the position of the output shaft if the cost for control effort were reduced to zero. One reason for this is that the specific solnic system described here was designed under the assumption that the cost of control effort would be significant, and therefore certain assumptions were built into the simulation which would not be valid for the zero-cost-for-control-effort case. For, one example, the last two terms of equation (6-1) were neglected. For another, the cost-optimization scheme which is outlined in section 6.2 and figure (7-1) would be inappropriate if the cost of control effort, a_c, in equation (6-4) were set to zero. It would be an interesting task to determine what the ultimate accuracy limit would be if the solnic system were modified in an optimal manner for the case in which a_c has a value of zero. In particular, it would be interesting to determine how the solnic system would compare with a dithered linear system.

The mode-identification decision makers used in the simulation were not optimal but they produced good results. The question

as to how much better the results would have been if the decision makers had been optimal remains unanswered. The whole area of mode estimation is relatively unexplored.

There is a need for some theorems and solutions defining the optimal compromise in relationship to the identification-singularity versus cost-nonoptimality dilemma.

A study which could have tremendous practical potential is that of extending the solnic concept to apply to real physical plants which have stochastic torques as well as nonlinear friction at the output shaft.

KEYED BIBLIOGRAPHY

(1) Hamming, R. W., Numerical Methods for Scientists and Engineers, New York: McGraw-Hill, 1962.

(2) Smith, Otto, Feedback Control Systems, New York: McGraw-Hill, 1958.

(3) Korn, G. A., and T. M. Korn, Electronic Analog Computers, New York: McGraw-Hill, 1956.

(4) Lauer, H., R. Lesnick, and L. E. Matson, Servomechanism Fundamentals, New York: McGraw-Hill, 1947.

(5) Gibson, J. E., and F. B. Tuteur, Control System Components, New York: McGraw-Hill, 1958.

(6) Bohacek, P. K., and F. B. Tuteur, "Stability of Servomechanisms with Stiction and Friction in the Output Element," IRE Transactions on Automatic Control, May 1961, pp 222-229.

(7) Swamy, M. N. S., "The Steady State Response of a Servosystem Taking Stiction and Coulomb Friction into Consideration," Journal of the Franklin Institute, Sept 1965, pp 205-221.

(8) Zheletsov, N. A., "Metod Tochechnovo Preobrazovaniya i Zadacha Ovynuzdennykh Kolebaniyakh Ostsillyatora c 'Kombinirovannym' Trenim [Transform Method and Problems Concerning Fluctuating Oscillations with Coulomb Friction]," Applied Mathematics and Mechanics 13, 3-40, Institute of Mechanics Academy, Nauk, U.S.S.R., 1949.

(9) Biernson, George, "Relation Between Structural Compliance and Allowable Friction in a Servomechanism," IEEE Transactions on Automatic Control, Jan 1965, pp 59-66.

(10) Booton, R. C. Jr., "The Analysis of Nonlinear Control Systems with Random Inputs," Proceedings of the Symposium on Nonlinear Circuit Analysis, New York, N.Y., April 23, 24, 1953 Volume II, New York: Interscience Publishers, Inc., 1953, pp 369-391.

(11) Pervozvanskii, A. A., Random Processes in Nonlinear Control Systems, New York: Academic Press, 1965.

(12) Gantmacher, F. R., Applications of Matrix Theory, New York: Interscience Publishers, Inc., 1959.

(13) Witsenhausen, H. S., "A Class of Hybrid-State Continuous Time Dynamic Systems," IEEE Transactions on Automatic Control, April 1966, pp 161-167.

(14) Faddeeva, V. N., Computational Methods of Linear Algebra, New York: Dover Publications, Inc., 1959.

(15) Detchmendy, D. M., and R. Sridhar, "Sequential Estimation of States and Parameters in Noisy Non-Linear Dynamical Systems," 1965 Joint Automatic Control Conference (Preprint), pp 56-63.

(16) Sworder, David, Optimal Adaptive Control Systems, New York: Academic Press, 1966.

(17) Lee, R. C. K., Optimal Estimation, Identification, and Control, Cambridge, Mass.: The M.I.T. Press, Research Monograph No. 28, 1964.

ADDITIONAL BIBLIOGRAPHY

Chang, S. L. S., Synthesis of Optimum Control Systems, New York: McGraw-Hill, 1961.

Chestnut, H., and R. Mayer, Servomechanisms and Regulating System Design, New York: John Wiley & Sons, 1951.

Fisher, J. R., Optimal Nonlinear Filtering, Los Angeles, University of California Department of Engineering Report No. 66-5, January 1966.

Ho, Y. C., and R. C. K. Lee, "A Bayesian Approach to Problems in Stochastic Estimation and Control," IEEE Transaction on Automatic Control, October 1964, pp 333-339.

Karplus, W. J., and W. W. Soroka, Analog Methods Computation and Simulation, New York: McGraw-Hill, 1959.

Lavi, A., and J. C. Strauss, "Parameter Identification in Continuous Dynamic Systems," 1965 IEEE International Convention Record, Part 6, March 1965, pp 49-61.

Mayer, Arthur, "Analysis of Gyro Orientation," IRE Transactions on Automatic Control, Dec 1958, pp 93-101.

Minorsky, Nicholas, Nonlinear Oscillations, Princeton, New Jersey: D. Van Nostrand Company, Inc., 1962.

Newton, Gould, and Kaiser, Analytical Design of Linear Feedback Controls, New York: John Wiley, 1957.

Parvin, Richard H., Inertial Navigation, New York: D. Van Nostrand Company, Inc., 1962.

Sage, A. P., and B. R. Eisenberg, "Experiments in Nonlinear and Nonstationary System Identification via Quasilinearization and Differential Approximation," 1966 Joint Automatic Control Conference (Preprint), pp 522-530.

Tou, Julius T., Digital and Sampled-data Control Systems, New York: McGraw-Hill, 1959.

Truxal, John G., Automatic Feedback Control System Synthesis, New York: McGraw-Hill, 1955.

Wilcox, J. C., "Self-Contained Orbital Navigation Systems with Correlated Measurement Errors," AIAA/ION Guidance and Control Conference, Minneapolis, Minn.: August 1965, pp 231-247.

BIOGRAPHICAL SKETCH

William Fred Acker was born in Springfield, Missouri, on May 8, 1930. He graduated magna cum laude in June, 1952, with the degree of Bachelor of Engineering with major in Mechanical Engineering from Vanderbilt University where he became a member of Tau Beta Pi. He went to work for Honeywell on June 10, 1952, for the second time and has been either employed by them or on leave of absence from them continuously since that date. By taking courses at night, obtaining a Honeywell fellowship, and finally by living of off savings, he succeeded in obtaining the degree of Master of Science in Electrical Engineering from the University of Minnesota in June, 1955. On May 13, 1955, prior to official receipt of his degree, he was inducted into the army as a private. On his first leave, he returned to Minneapolis to marry Miss Betty Marie Hokanson who was then taking graduate work in home economics at the University of Minnesota.

He and Miss Hokanson were married on July 27, 1955. They spent the next two years at Las Cruces, New Mexico, near White Sands Missile Testing Center where PFC Acker served as reliability, modification, and field-change engineer for the NIKE missile and associated tactical equipment. At night, Mr. Acker taught descriptive geometry at the New Mexico College of Agriculture and Mechanic Arts. He also

took graduate courses there in thermodynamics, and jet and rocket engines.

In June, 1957, he resumed working for Honeywell at the Minneapolis Aero Division, where he worked on aircraft hydraulic servocylinders and on the CF 105 inertial-guidance platform. Honeywell transferred him to the St. Petersburg, Florida Aero Division in October 1958, where he worked as a platform servo analyst for many inertial-guidance projects including the GEMINI inertial measuring unit and the first airborne platform with electrically suspended gyros. It was during this period that he and Leo Spiegel co-invented the DYNAGON, the 22-bit digital angle pickoff used on the airborne ESG platform. It was also during this period that he and his wife adopted two children: Steven William, born December 31, 1959; and Lisa Ruth, born March 5, 1961.

In September, 1963, having obtained a NASA fellowship and a leave of absence from Honeywell, Mr. Acker enrolled at the University of Florida as a full-time student and began working toward his doctorate. Having completed his course work and expended his fellowship, he returned to Honeywell in St. Petersburg in September, 1965, and worked there about three days per week on an hourly wage basis while commuting to Gainesville to complete his dissertation. Meanwhile at Honeywell, he analytically studied the drift of electrically suspended gyroscopes, and system mechanizations, and the alignment and navigation equations related to these gyros. In March, 1967, he

was transferred to the Advanced Communications Division where he is presently working on theoretical problems concerning adaptive transversal equalizers for improving the transmission of digital data through telephone circuits.

This dissertation was prepared under the direction of the chairman of the candidate's supervisory committee and has been approved by all members of that committee. It was submitted to the Dean of the College of Engineering and to the Graduate Council, and was approved as partial fulfillment of the requirements for the degree of Doctor of Philosophy.

April, 1967

Dean, College of Engineering

Dean, Graduate School

Supervisory Committee:

Chairman

5030